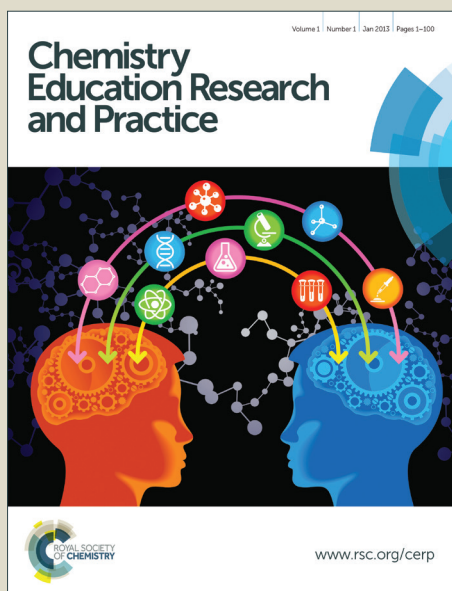


Chemistry Education Research and Practice

Accepted Manuscript



This is an *Accepted Manuscript*, which has been through the Royal Society of Chemistry peer review process and has been accepted for publication.

Accepted Manuscripts are published online shortly after acceptance, before technical editing, formatting and proof reading. Using this free service, authors can make their results available to the community, in citable form, before we publish the edited article. We will replace this *Accepted Manuscript* with the edited and formatted *Advance Article* as soon as it is available.

You can find more information about *Accepted Manuscripts* in the [Information for Authors](#).

Please note that technical editing may introduce minor changes to the text and/or graphics, which may alter content. The journal's standard [Terms & Conditions](#) and the [Ethical guidelines](#) still apply. In no event shall the Royal Society of Chemistry be held responsible for any errors or omissions in this *Accepted Manuscript* or any consequences arising from the use of any information it contains.

Rabbit-ears hybrids, VSEPR sterics, and other orbital anachronisms

Allen D. Clauss,^{a,c} Stephen F. Nelsen,^a Mohamed Ayoub,^b John W. Moore,^{a,d}
Clark R. Landis,^{a,e} and Frank Weinhold^{*a,f}

^aDepartment of Chemistry, University of Wisconsin, Madison, WI 53706, USA.

^bDepartment of Chemistry, UW-Washington Co., West Bend, WI 53095, USA. E-mail:

mohamed.ayoub@uwc.edu. ^cPresent address: Xolve, Inc. 1600 Aspen Commons

#101, Middleton, WI 53562. E-mail: clauss@chem.wisc.edu. ^dE-mail:

jwmoore@chem.wisc.edu. ^eE-mail: landis@chem.wisc.edu. ^fE-mail:

weinhold@chem.wisc.edu.

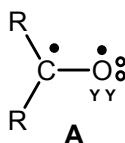
ABSTRACT: We describe the logical flaws, experimental contradictions, and unfortunate educational repercussions of common student misconceptions regarding the shapes and properties of lone pairs, inspired by overemphasis on “valence shell electron pair repulsion” (VSEPR) rationalizations in current freshman-level chemistry textbooks. VSEPR-style representations of orbital shape and size are shown to be fundamentally inconsistent with numerous lines of experimental and theoretical evidence, including quantum mechanical “symmetry” principles that are sometimes invoked in their defense. VSEPR-style conceptions thereby detract from more accurate introductory-level teaching of orbital hybridization and bonding principles, while also requiring wasteful “unlearning” as the student progresses to higher levels. We include specific suggestions for how VSEPR-style rationalizations of molecular structure can be replaced with more accurate conceptions of hybridization and its relationship to electronegativity and molecular geometry, in accordance both with Bent’s rule and the consistent features of modern wavefunctions as exhibited by natural bond orbital (NBO) analysis.

Introduction

The first contact of many students of organic chemistry in the early 1960s with molecular orbital (MO) theory was through Streitwieser's influential book (Streitwieser, 1961). It mainly covered Hückel-type calculations in which non-carbon atoms are only treated by changes of α and β parameters. Other complicating factors — such as the existence or spatial positioning of H atoms, lone pairs, or the skeletal sigma-bonding framework — were ignored entirely. “Lone pair” is not even an entry in the book's index.

Howard Zimmerman (1963) recognized the importance of distinguishing between the hybridized and unhybridized lone pairs at the carbonyl oxygen for understanding ketone photochemistry. He employed “circle-dot-y” notation for carbonyl groups, in

1
2
3
4 which the s-rich lone pair (collinear with the CO axis) is shown as small circles, the
5 out-of-plane π_{CO} electrons as a pair of dots, and the unhybridized in-plane p-type lone
6 pair as a pair of y's, as shown in A.
7



14 As pointed out by Jorgensen and Salem (1973) in their book that informed a
15 generation of organic chemists about more realistic details of electronic orbitals:
16

17
18 *If we are seeking favorable intramolecular interactions between lone-pairs and other*
19 *orbitals, it is absolutely necessary to consider those lone pair orbitals which have the*
20 *proper local symmetry.*
21
22

23 Although the importance of distinguishing between lone pairs of different symmetry
24 was clearly stated over forty years ago, the distinction appears to have been widely
25 ignored by subsequent organic and general chemistry textbook authors. Instead, the
26 widespread teaching of valence shell electron-pair repulsion (VSEPR) theory has
27 fostered an unfortunate tendency to envision lone pair MOs of improper local
28 symmetry. VSEPR was introduced by Gillespie and Nyholm (1957) as a simplified
29 way to envision heteroatom lone pairs in molecular skeletal structure [see the
30 historical context provided in an early pedagogical review by Gillespie (1963)].
31 According to VSEPR theory, two equivalent “rabbit-ears” lone pairs are directed
32 above and below the skeletal bonding plane at approximately tetrahedral angles for
33 disubstituted group-16 (chalcogen) atoms, and three equivalent “tripod” lone pairs are
34 similarly directed around monosubstituted group-17 (halogen) atoms. As we
35 emphasize below, such “equivalent” (equal-energy, tetrahedrally hybridized and
36 oriented) depictions of lone pairs cannot be consistent with the local σ - π electronic
37 symmetry of the skeletal bonding framework.
38
39
40
41
42
43

44 Deliberate teaching of incorrect conceptions of lone pairs and their purported “steric
45 demands” that must be unlearned as students progress to deeper understanding of
46 structure and bonding cannot be efficient or desirable (Schreiner, 2002). Although it
47 is widely conceded that MO theory is required for proper understanding of molecular
48 structure and bonding, VSEPR-type textbook illustrations of lone pairs often appear in
49 close proximity to introductory MO concepts with which they are logically and
50 mathematically incompatible. It has been steadfastly maintained by Gillespie and
51 others that equal-energy lone pairs are “mathematically equivalent” to the proper s-
52 rich and pure-p lone pairs (Gillespie, 1974), (Gillespie, 2004), but this is certainly
53 untrue except at such low levels of theory as not to warrant serious current
54 consideration (for mathematical aspects of this purported equivalency, see Appendix
55 1). Although problems with VSEPR rationalizations have been pointed out repeatedly
56
57
58
59
60

1
2
3
4 in the chemical education literature (Walsh, 1953), (Laing, 1987), (Clauss and Nelsen,
5 2009), many textbook authors and teachers remain firmly committed to teaching
6 rabbit-ears/VSEPR structural and steric concepts that we believe are scientifically
7 unjustifiable.
8

9
10 To clarify the relationship between localized Lewis structure (lone pair/bond pair)
11 and delocalized MO descriptions of molecular electronic structure, we make frequent
12 use of natural bond orbitals (NBOs) (Weinhold and Landis, 2012) or the closely
13 related natural localized molecular orbitals (NLMOs) (Reed and Weinhold, 1985); for
14 an overview of “natural”-type orbitals, see
15 http://nbo6.chem.wisc.edu/webnbo_css.htm. NBOs are a unique,¹ intrinsic, and
16 complete set of orthonormal orbitals that optimally express the localized Lewis-like
17 aspect of the wavefunction and are readily obtained for arbitrary wavefunctions as
18 well as density functional and perturbative treatments of MO or correlated type. The
19 leading Lewis-type NBOs/NLMOs have a one-to-one mapping onto the localized
20 structural elements of the Lewis dot diagram, allowing them to serve as ideal basis
21 functions to re-express MOs in the language of structural chemists. The pedagogical
22 advantages of localized NBO vs. delocalized MO description are described more fully
23 in a variety of journal articles (Weinhold and Landis, 2001), (Weinhold, 2012),
24 (Weinhold and Klein, 2014), web-based tutorials
25 (http://nbo6.chem.wisc.edu/tut_cmo.htm), and monographs (Weinhold and Landis,
26 2005), (Weinhold and Landis, 2012). Ready availability of *WebMO*
27 (<http://www.webmo.net/>) and other web-based computational utilities (e.g.,
28 <http://www.youtube.com/watch?v=Hzpr74WbDPo>) makes calculation and
29 visualization of these orbitals increasingly practical for laptop-toting students in the
30 modern wi-fi classroom or laboratory (see, e.g.,
31 [https://www.chem.wisc.edu/content/experiment-5-computational-molecular-](https://www.chem.wisc.edu/content/experiment-5-computational-molecular-modeling-webmo)
32 [modeling-webmo](https://www.chem.wisc.edu/content/experiment-5-computational-molecular-modeling-webmo)).
33
34
35
36
37
38
39
40
41

42 **Are the lone pairs of water “equivalent”?**

43
44 As described in Appendix 1, the idea that VSEPR-type lone pairs are
45 “mathematically equivalent” to distinct s-rich and pure-p lone pairs of water rests on
46 superficial understanding of Fock's theorem (Fock, 1930) concerning the unitary
47
48

49
50 ¹ As noted below, the choice of “MOs” can be rather arbitrary, insofar as *any* unitary transformation of
51 MOs leads to the same single-determinant wavefunction with *no* effect on the energy or other observable
52 properties of the system. MOs therefore provide no criterion for which unitarily-equivalent set is
53 considered “best,” because all satisfy the full double-occupancy condition. In contrast, NBOs are
54 *uniquely* determined by the form of the wavefunction (whether of MO or more complex form) because
55 each Lewis-type NBO generally has *distinct* occupancy (<2), reflecting the fact that *some* occupancy must
56 appear in non-Lewis NBOs to represent the physical effects of resonance-type delocalizations. The
57 fundamental maximum-occupancy criterion of all “natural”-type methods therefore dictates uniquely
58 which choice of NBOs is optimal, and by how much. Moreover, these NBOs are found to converge
59 rapidly to unique limiting forms as the wavefunction approaches exactness.
60

1
2
3
4
5
6
7
8
9
10
11
12
13
14
15
16
17
18
19
20
21
22
23
24
25
26
27
28
29
30
31
32
33
34
35
36
37
38
39
40
41
42
43
44
45
46
47
48
49
50
51
52
53
54
55
56
57
58
59
60

equivalence of doubly-occupied localized (LMOs) vs. canonical MOs (CMOs) in single-determinant Hartree-Fock (HF) or density functional (DFT) approximations. However, at any reasonable level of MO theory, the lone pair MOs of water (whether of canonical or optimally localized NLMO form) are found to be quite *distinct* and *inequivalent*, both in form and energy. Whether one can find *some* unitary mixture of lone-pair MOs that gives resulting equal-energy orbitals is essentially irrelevant. Indeed, one could equally well find such an equal-energy mixture of core and valence-type MOs, but this provides no real justification for claiming that core and valence orbitals are somehow “equivalent.”

Figure 1 displays 3-d surface plots of lone-pair-type MOs for H₂O at diverse DFT, HF, and semi-empirical levels, illustrating their essential visual similarity to MO images of Jorgensen and Salem (1973) and *dissimilarity* to VSEPR-style cartoon images. The selected DFT and HF levels span a wide range of accuracy for treating details of chemical interactions, but *all* concur on such qualitatively important features as the inequivalent shapes and energetics of lone pairs.

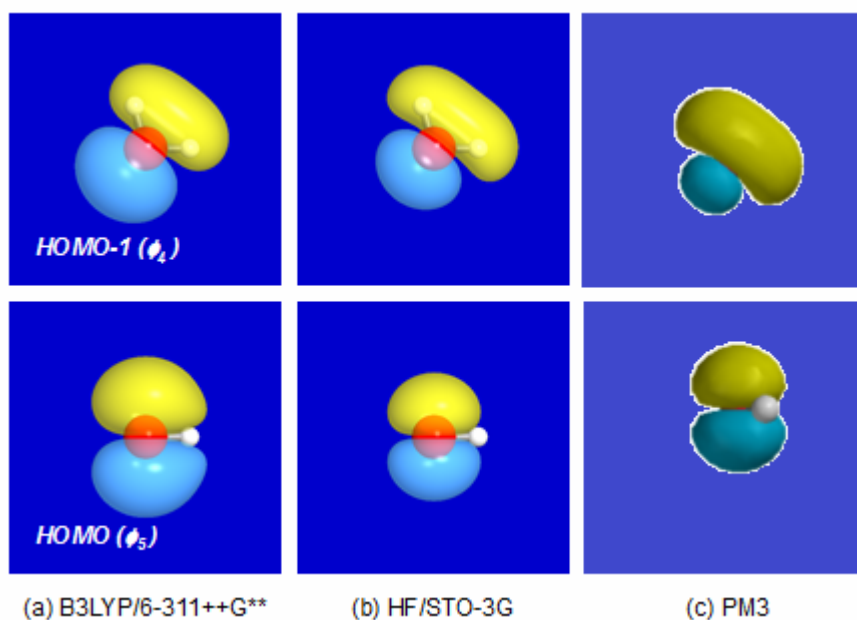


Figure 1. Highest occupied (lone pair-like) MOs of water at various DFT, Hartree-Fock, and semi-empirical MO levels (as labeled), showing distinct σ -type (ϕ_4) and π -type (ϕ_5) orientation and shape at each level: (a) hybrid density functional (B3LYP) method at augmented triple-zeta basis level; (b) Hartree-Fock at minimal basis level; (c) semi-empirical “PM3” model of Dewar type. See Foresman and Frisch (1996) for more complete description of methods and basis sets used herein.

Figure 2 shows additional radial and angular details of MO vs. NBO lone pairs in 2-d contour plots for H₂O, comparing lone pair-type MOs (Fig. 2a) with the uniquely

determined s-rich ($n_{\text{O}}^{(\sigma)}$) and pure-p ($n_{\text{O}}^{(\pi)}$) lone-pair NBOs (Fig. 2b) at each level. The essential differences in lone pair hybridization are seen most clearly in the NBO plots, whereas MOs tend to form somewhat confusing mixtures of 1-center lone pair orbitals with symmetry-adapted combinations from other centers, as discussed below.

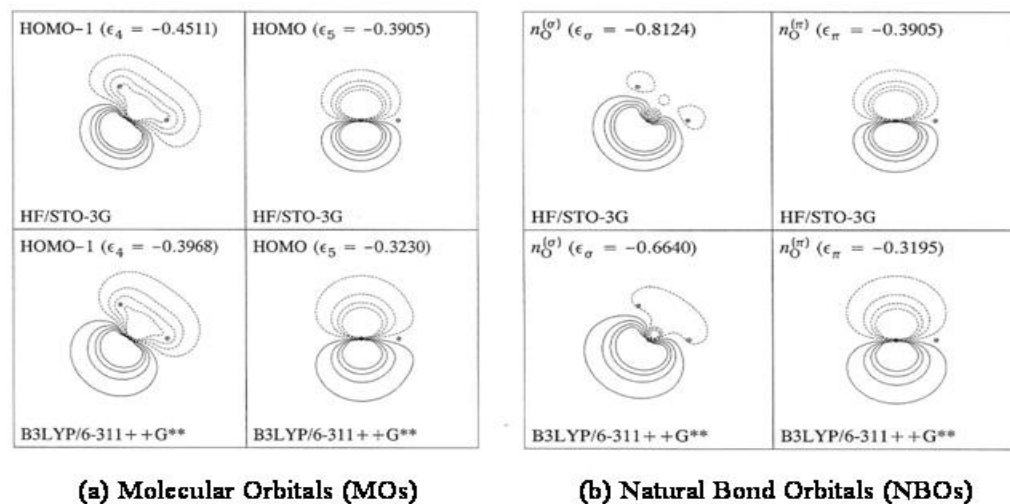


Figure 2. 2-d contour plots comparing (a) MOs and (b) NBOs for lone pairs of water at HF/STO-3G and B3LYP/6-311++G** levels, showing strong inequivalencies of hybridization, energy and shape. The chosen contour plane lies within (for σ -type orbitals) or perpendicular to (for π -type orbitals) the plane of nuclei marked by crosshairs.

Mathematically and group theoretically, one can easily see (Weinhold and Landis, 2005, p. 52ff) that atomic s-p symmetries can only be broken by chemical bonding interactions, and these cannot involve p-orbitals outside the line (for diatomics) or plane (for triatomics) of chemical bonding. Thus for H_2O , the pure p_z (out-of-plane) lone pair must always remain distinct from the s-rich hybridized lone pair in the xy-plane of skeletal bonding. The CMOs, NBOs, or NLMOs of H_2O must therefore exhibit the strict σ/π separation (as irreducible representations of C_{2v} symmetry) that distinguishes the unhybridized π -type $n_{\text{O}}^{(\pi)}$ (pure p_z) lone pair from the hybridized σ -type $n_{\text{O}}^{(\sigma)}$ ($\sim sp^2$) lone pair in the molecular plane. Even if the in-plane $n_{\text{O}}^{(\sigma)}$ were to unaccountably lose all s-character, in gross violation of Bent's rule (Bent, 1961), the orientations and energies of $n_{\text{O}}^{(\sigma)}$, $n_{\text{O}}^{(\pi)}$ must still differ *qualitatively* from those of VSEPR-style rabbit ears.

As Fock's theorem suggests, slightly different CMO mixings may be manifested by different levels of MO theory, such as the low-level HF/STO-3G (minimal basis HF) and higher-level B3LYP/6-311++G** (extended-basis DFT) levels displayed in Fig. 2. This confuses the issue slightly, because the delocalized HOMO-1 ϕ_4 will contain

1
2
3 somewhat different unitary mixtures of the $n_{\text{O}}^{(\sigma)}$ lone-pair NBO with the in-phase
4 combination of σ_{OH} , $\sigma_{\text{OH}'}$ bond NBOs. For the MOs of Fig. 2, these mixtures are
5 given by
6
7

8
9 (1a) $\varphi_4 = 0.79n_{\text{O}}^{(\sigma)} + 0.43(\sigma_{\text{OH}} + \sigma_{\text{OH}'}) + \dots$ (HF/STO-3G)

10
11 (1b) $\varphi_4 = 0.86n_{\text{O}}^{(\sigma)} + 0.36(\sigma_{\text{OH}} + \sigma_{\text{OH}'}) + \dots$ (B3LYP/6-311++G**)

12
13 corresponding to 62% vs. 74% lone-pair character for HF/STO-3G vs. B3LYP/6-
14 311++G**, respectively. However, as shown in Fig. 2, the energies and shapes of
15 underlying $n_{\text{O}}^{(\sigma)}$, $n_{\text{O}}^{(\pi)}$ NBOs are quite distinct at each level and highly transferable
16 from one level to another. These numerical examples make it clear, consistent with
17 the group-theoretical arguments of the preceding paragraph and mathematical analysis
18 given in Appendix 1, that $n_{\text{O}}^{(\sigma)}$, $n_{\text{O}}^{(\pi)}$ lone pairs cannot exhibit VSEPR-type
19 “equivalency” at *any* theoretical level of useful chemical accuracy.²
20
21
22
23

24 25 **Does the local symmetry of inequivalent lone pairs persist in** 26 **larger molecules?** 27

28
29 Although the inequivalency of $n_{\text{O}}^{(\sigma)}$, $n_{\text{O}}^{(\pi)}$ lone pairs is dictated by strict triatomic
30 C_{2v} symmetry in water, one might question whether similar σ/π separation (“effective”
31 local symmetry) is manifested in larger molecules. Many examples might be cited to
32 demonstrate that this is generally so. Here we briefly mention three representative
33 organic compounds containing disubstituted oxygen whose structural/reactive
34 properties support the (computationally unambiguous) picture of inequivalent $n_{\text{O}}^{(\sigma)}$,
35 $n_{\text{O}}^{(\pi)}$ oxygen lone pairs and rule out conflicting VSEPR/rabbit-ears conceptions.
36
37
38
39

40 Figure 3 compares 3-d visual images of the oxygen lone pair NBOs of water with
41 those of methanol, formic acid, and furan, all at B3LYP/6-311++G** level. The
42 visual orbital images appear virtually indistinguishable, confirming the high
43 transferability of $n_{\text{O}}^{(\sigma)}$, $n_{\text{O}}^{(\pi)}$ local-symmetry NBOs into larger species.
44
45
46
47
48
49
50
51
52
53
54

55 ²Note that this remark extends also to multi-configurational GVB (Generalized Valence Bond)
56 wavefunctions, which (even if employing rabbit-ear orbitals as initial guesses) are also found to converge
57 self-consistently to lone-pair NBOs of clearly *inequivalent* form, similar to those of other methods
58 discussed above.
59
60

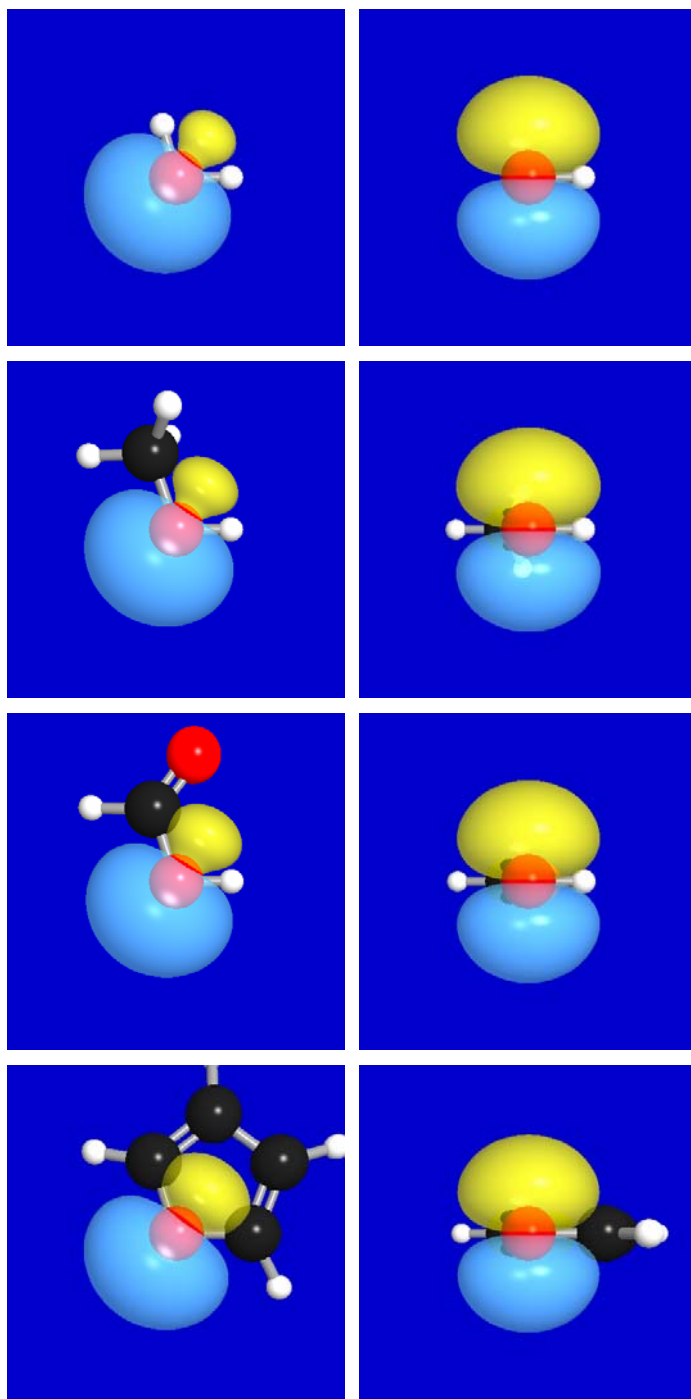


Figure 3. 3-d surface plots of $n_O^{(\sigma)}$ (left), $n_O^{(\pi)}$ (right) lone pairs for (a) water, (b) methanol, (c) formic acid, and (d) furan (B3LYP/6-311++G** level).

Table 1 displays the explicit mathematical relationships between MOs and NBOs [analogous to Eqs. (1a,b) for water] for the alternative CH₃OH, HCOOH, and furan species of Fig. 3. As the table shows, the high-lying MOs exhibit somewhat different mixings of intrinsic lone pair and bond NBOs in each species, but despite such confusing mixing (of no physical consequence), the MOs of highest lone-pair parentage all exhibit $n_{\text{O}}^{(\sigma)}$, $n_{\text{O}}^{(\pi)}$ -type inequivalencies similar to those of Figs. 1, 2. Thus, computational results for larger molecules consistently confirm the strong tendency to preserve effective local $n_{\text{O}}^{(\sigma)}$, $n_{\text{O}}^{(\pi)}$ (C_{2v} -like) character in all such species.

species	MO	NBO composition
CH ₃ OH	ϕ_8	$0.68 n_{\text{O}}^{(\sigma)} - 0.43\sigma_{\text{CH}} - 0.33\sigma_{\text{OH}} + \dots$
	ϕ_9	$0.89 n_{\text{O}}^{(\pi)} + 0.32(\sigma_{\text{CH}'} - \sigma_{\text{CH}'}) + \dots$
HCOOH	ϕ_{10}	$0.64 n_{\text{O}}^{(\sigma)} - 0.47 n_{\text{O}}^{(\sigma)} - 0.36\sigma_{\text{CH}} + \dots$
	ϕ_{11}	$0.71 n_{\text{O}}^{(\pi)} - 0.67\pi_{\text{CO}} + \dots$
furan	ϕ_{12}	$0.80 n_{\text{O}}^{(\pi)} + 0.41(\sigma_{\text{C(4)C(7)}}) + \dots$
	ϕ_{15}	$0.60 n_{\text{O}}^{(\sigma)} - 0.43(\sigma_{\text{C(3)H}} + \sigma_{\text{C(4)H}}) - 0.39\sigma_{\text{C(3)C(4)}} + \dots$

Table 1. NBO composition of “most lone pair-like” MOs (from CMO keyword option) in methanol, formic acid, and furan [cf. text Eq. (1b) for water], showing leading mixings with parent $n_{\text{O}}^{(\sigma)}$, $n_{\text{O}}^{(\pi)}$ NBOs.

What does experimental evidence tell us about lone pairs?

Aside from the clear computational picture, the characteristics of lone pairs can also be inferred from experimental evidence concerning their observed effects on molecular properties. Many contradictions are encountered in attempts to apply VSEPR-style reasoning to rationalize experimental properties of known compounds containing disubstituted oxygen or sulfur, examples of which will be summarized in this section.

One well-known “textbook example” is provided by the dipole analysis of hydroxylamine conformers by Jones *et al.* (1974). These workers measured the dipole moment of trimethylhydroxylamine to be 0.88 Debye and attempted to analyze its rotameric conformations about the NO bond by the VSEPR-inspired rabbit-ear lone pair analysis as shown in Figure 4. Using simple bond-dipole additivity relationships based on other known compounds (because this was still at a time when organic chemists could not routinely perform the required electronic structure calculations!),

these workers estimated the dipole moments for conformers **B**, **C**, and **D**, as shown in the figure. Because the observed dipole moment was less than that estimated for the staggered structures **C** and **D**, they concluded that eclipsed structure **B** must be present. Because **C** has “large” lone pairs crowded together, its contribution was neglected, and the molecule was concluded to be approximately a 3:1 mixture of **D**:**B**.

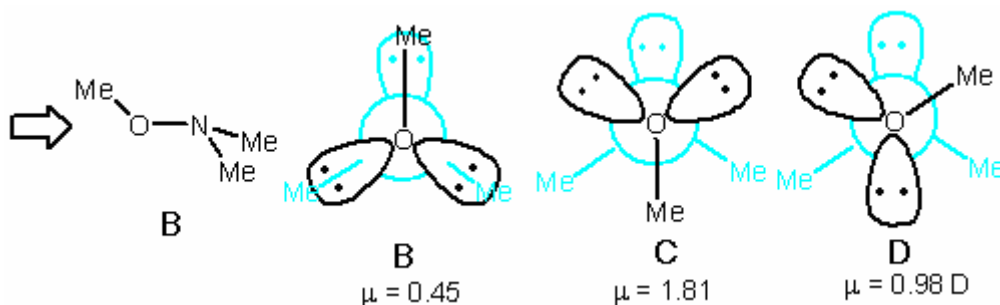


Figure 4. VSEPR-type rabbit-ears cartoons for trimethylhydroxylamine conformers in Newman projections (with arrow showing view direction, and rear NMe_2 group in light blue).

However, this conclusion is fundamentally incorrect (Nelsen *et al.*, 1987), and the error can be traced to the rabbit-ear lone pair representation that was used. Similar analysis using the proper $n_{\text{O}}^{(\sigma)}$ and $n_{\text{O}}^{(\pi)}$ lone pairs is shown in Figure 5. **B** and **C** are energy minima, but **B** is no longer “eclipsed,” and **D** (selected as the most important contributor by rabbit-ears analysis) is not even an energy minimum! (Even semi-empirical calculations get this right, because they use proper lone pairs.) As shown more clearly in the first figure of Riddell's (1981) review of hydroxylamine geometries, **D** lies on the side of a hill on the energy surface for ON rotation, so it cannot be contributing to the observed dipole moment because no significant amount is present. The s-rich lone pairs are shown close to oxygen in Fig. 5, because they are so compact and low in energy as to have no significant interaction with adjacent methoxy substituents, and therefore make no significant contribution to the torsional energy surface.

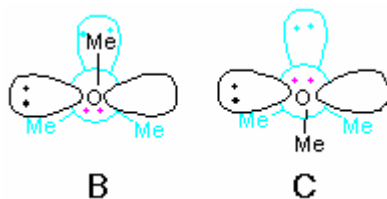


Figure 5. Similar to Fig. 4, for proper p-rich (black lobes) and s-rich (magenta dots) lone pairs at oxygen.

Still more striking experimental contradictions to VSEPR-inspired rabbit-ears conceptions are provided by sulfur compounds, including the ubiquitous CSSC disulfide structural motifs of proteins and peptides. Early structural understanding of such species came from electron diffraction measurements on HSSH (Winnewisser *et al.*, 1968), (Hahn *et al.*, 1998), MeSSMe (Sutter *et al.*, 1965), (Yokozeki and Bauer, 1976), (Beagley and McAloon, 1971), ClSSCl (Beagley *et al.*, 1969), (Kniep *et al.*, 1983), and FSSF (Kuczkowski, 1964), (Marsden *et al.*, 1989), but because organic and biochemists were unfamiliar with such techniques, the significance of the work was too long overlooked. Here again the use of rabbit-ears lone pairs leads to misunderstanding. As shown in Figure 6, the VSEPR-inspired view of disulfide linkages (with each sulfur bearing “bulky” rabbit-ears lone pairs at tetrahedral angles) would lead to the expectation of XSSX dihedral angle $\theta = 180^\circ$, to minimize “steric clashes” between lone pairs. Alternatively, if anomeric $n_S-\sigma^*_{SH}$ interactions are judged most important, the tetrahedral rabbit-ears orientation predicts a preferred $\theta \cong 60^\circ$ conformation. However, neither expectation is correct! The preferred θ is found to be near 90° for all the above examples (as the inequivalent $n_S^{(\sigma)}$, $n_S^{(\pi)}$ model suggests), and the correct result is calculated even by simple semi-empirical methods that incorporate the necessary lone pair inequivalencies originally pointed out by Jorgensen and Salem (1973).

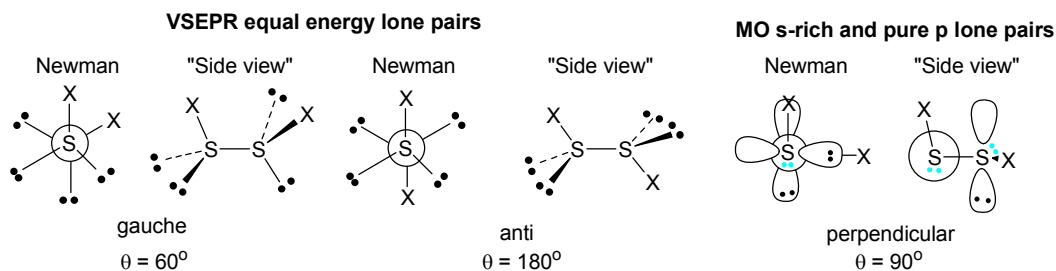


Figure 6. Expected conformers of XSSX compounds in VSEPR (left) vs. MO (right) lone-pair formulations.

The disulfide species are also instructive with regard to the seemingly unending debates about steric vs. hyperconjugative effects in torsional phenomena (Bickelhaupt and Baerends, 2003), (Weinhold, 2003). It had been common (Steudel, 1975) to rationalize the $\theta \cong 90^\circ$ conformational preference of disulfides in terms of a “4e-repulsive” interaction between vicinal $n_S^{(\pi)}$ lone pairs. However, structural data strongly suggest that the 90° preference arises because the high-energy pure-p $n_S^{(\pi)}$ lone pair is thereby able to align most favorably with vicinal σ^*_{SH} acceptor orbitals for maximal $n_S^{(\pi)}-\sigma^*_{SH}$ hyperconjugative stabilization. If the hyperconjugative model is correct, one ought to see characteristic SS bond length variations reflecting $n_S^{(\sigma)}-\sigma^*_{SX}$ attraction, and therefore sensitive to X *electronegativity* (rather than “steric bulk”)

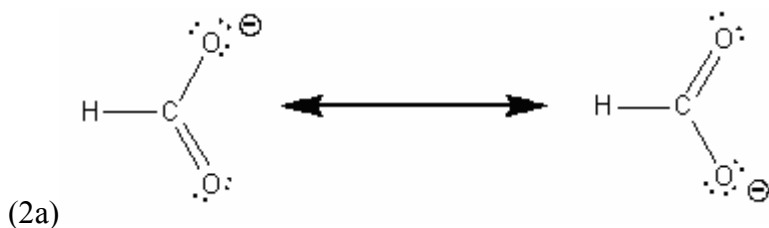
1
2
3
4
5
6
7
8
9
10
11
12
13
14
15
16
17
18
19
20
21
22
23
24
25
26
27
28
29
30
31
32
33
34
35
36
37
38
39
40
41
42
43
44
45
46
47
48
49
50
51
52
53
54
55
56
57
58
59
60

variations. This is indeed found to be the case, with experimental SS bond lengths of 2.056 Å for HSSH, 2.029 Å for MeSSMe, 1.943 Å for ClSSCl, and 1.890 Å for FSSF. Similar resolutions of steric vs. hyperconjugative controversies are found for hydrazines (Petillo and Lerner, 1993), peroxides (Carpenter and Weinhold, 1988), and numerous other species (Pophristic and Goodman, 2001).

Other pedagogical dilemmas of using VSEPR-derived lone pairs

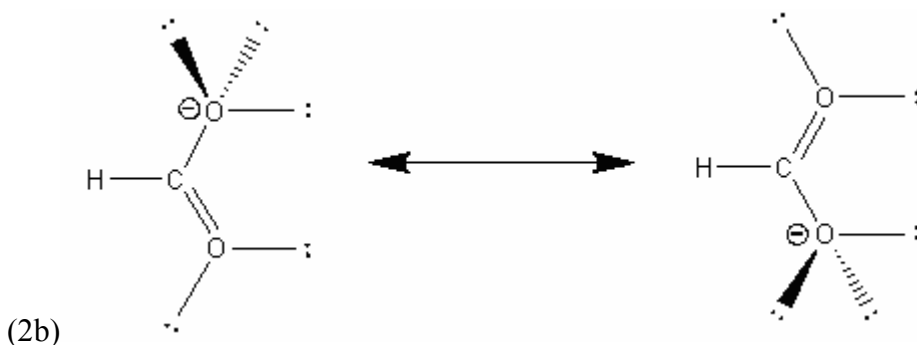
As known from many studies of stereochemical and anomeric phenomena (DeLongchamps, 1983), (Kirby, 1983), lone pairs commonly act as powerful electronic donors (Lewis bases) in conjugative and hyperconjugative donor-acceptor interactions. Many details of structure and reactivity are therefore *sensitive* to lone pair shape, energy, and orientation, enabling one to clearly distinguish equivalent (rabbit ears) from inequivalent ($n_{\text{O}}^{(\sigma)}/n_{\text{O}}^{(\pi)}$) lone pairs. This has important implications in how we teach about lone pairs in general chemistry and introductory organic chemistry. The current common practice of using VSEPR to predict and explain electronic structure, particularly the spatial orientation of lone pair electrons, results in a need to start “unteaching” incorrect perceptions or having to use convoluted, invalid rationalizations almost immediately to help students work around their incorrect perceptions about lone pairs.

In introductory organic chemistry, contradictions with VSEPR arise early when students are introduced to the concept of resonance involving oxygen or nitrogen atoms conjugated to π systems. The contradictions go unnoticed by some (but not all) students and are glossed over by instructors who prefer not to start unteaching VSEPR immediately after it was covered. As a result, students are taught to draw resonance structures without considering the types of orbitals involved. If they do consider the types of orbitals, it becomes apparent that they are forming π -bonds using sp^3 orbitals. For example, when students learn about the acidity of carboxylic acids and the importance of resonance stabilization of carboxylate anions, they are taught to recognize resonance of the type shown in (2a) for the formate anion as being particularly stabilizing.



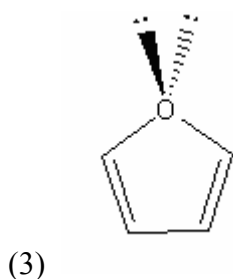
Using the VSEPR model, if students consider the orbitals involved in these resonance forms, then the lone pairs would have local symmetry as shown in (2b) which would

prevent any of the lone pairs on the anionic oxygen from forming a π -bond to the carbon atom.



Many instructors avoid addressing this contradiction, while others refer to the anionic oxygen “rehybridizing” to sp^2 allowing it to enter into resonance. Invoking such rehybridization arguments when there was no valid basis for considering the oxygen to be sp^3 hybridized to begin with is clearly a pedagogically unsound practice.

Whether or not such contradictions arise when the concept of resonance is first introduced, they invariably arise some weeks later when the structure and reactivity of conjugated and aromatic compounds are discussed in greater detail. For example, when discussing aromaticity, furan (C_4H_4O) is commonly cited as a heterocyclic compound that exhibits the classical chemical characteristics of aromaticity (Katritzky and Lagowski, 1967). However, students trained to use VSEPR consider the oxygen lone pairs in furan to be in equivalent sp^3 orbitals projecting above and below the plane of the ring as shown in (3),



which leads them to the logical conclusion that furan should not be aromatic because neither lone pair can be part of the π system of the ring. (If instead the rabbit-ears lone pairs are both counted as belonging to the π system, the usual $4n+2$ rule for aromaticity is again violated.) Many such conflicts can only be glossed over by inattention to orbital details.

Numerous related organic chemistry examples could be cited where VSEPR-inspired thinking leads to contradictions and incorrect conclusions. Indeed, most

1
2
3
4 conjugated systems containing heteroatoms tend to be viewed incorrectly by students
5 trained to use VSEPR, resulting in a range of incorrect perceptions about the structure,
6 stability, and reactivity of these systems. By the time students have completed one
7 semester of introductory organic chemistry, they have encountered so many of these
8 examples that their use of VSEPR to predict and explain electronic structure hurts
9 their understanding more often than it helps.
10
11

12
13 Still other pedagogical dilemmas are presented by the VSEPR-inspired concept that
14 lone pairs are sterically “repulsive” compared to bond pairs. Gillespie (1963)
15 recommended teaching that the tetrahedral hydride bond angles of methane were
16 reduced to observed values in ammonia (107.3°) and water (104.5°) because:
17
18

19 [lone pairs] *overlap with neighboring orbitals more extensively and therefore will*
20 *repel electrons in these neighboring orbitals more strongly than an electron pair in a*
21 *bonding orbital [with the result that] lone pair electrons will tend to move apart and*
22 *squash bonding electron pairs together*
23
24

25
26 Such language leads to the widespread perception that lone pairs are somehow
27 “effectively bigger” than bonding electron pairs. However, we may well ask what
28 evidence (other than mnemonic success of the VSEPR model itself) supports the
29 claim that lone pairs are effectively “bigger,” “more repulsive,” or “sterically
30 demanding” compared to bond pairs, or the assumption that moving lone pair
31 electrons apart (i.e., in the orthogonal xz-plane) should “squash” the σ_{OH} hydride
32 bonds to reduced angle in the molecular xy-plane of water.
33
34
35

36
37 On the experimental side, organic chemists often assess the relative size of
38 substituents by determining the equilibrium constant and Gibbs free energy difference
39 between the axial and equatorial conformers of a six-membered ring containing the
40 substituent (Anslyn and Dougherty, 2006). For any substituent larger than a hydride
41 bond, the conformation that places the bulky substituent in the equatorial position is
42 expected to be lower in energy, due to the unfavorable non-bonded 1,3 diaxial
43 interactions with CH bonds that occur when the substituent is in the axial position. As
44 shown in Figure 7, this method can be applied to piperidine ($\text{C}_5\text{H}_{10}\text{NH}$) to assess the
45 effective size of the nitrogen lone pair relative to the σ_{NH} hydride bond. Fig. 7
46 displays the experimental Gibbs free energy difference, +0.36 kcal/mol (Anet and
47 Yavari, 1977), which demonstrates that the n_{N} lone pair of piperidine definitely
48 prefers the *axial* position, and thus appears *smaller* than the σ_{NH} hydride bond by this
49 experimental criterion.³ Such experimental conflicts with VSEPR expectations
50 become increasingly numerous and troublesome as the student progresses to more
51 advanced levels.
52
53
54
55
56

57
58 ³ It should be noted that experimental cyclohexane A-factors may also involve significant axial-equatorial
59 differences in hyperconjugation, so they appear to be less reliable measures of “pure” steric effects than
60 other theoretical criteria described below.

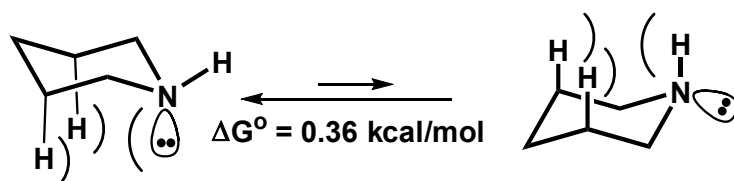


Figure 7. Gibbs free energy difference for axial vs. equatorial isomers of piperidine, indicating that the lone pair is effectively *smaller* than the hydride bond pair at nitrogen.

How *can* one satisfactorily explain X-O-Y bond angles without VSEPR?

As recognized by Pauling (1931), Slater (1931), Coulson (1958), and others, the basic origins of near-tetrahedral bond angles in main-group bonding lie in the *hybridization* concept. The subtle variations from tetrahedrality are similarly due to the subtle variations of hybridization (and therefore bond angle) with *electronegativity*, as expressed most succinctly in Bent's rule (Bent, 1961), viz.:

Central main-group atoms tend to direct bonding hybrids of higher p-character toward atoms of higher electronegativity

With this powerful mnemonic in hand, the student can easily employ elementary concepts of Lewis structure, periodic electronegativity trends, and bond hybrid vs. angle relationships to make VSEPR-style predictions of molecular structure with confidence and accuracy.

The fundamental relationship between main-group hybrids [e.g., hybrids sp^{λ_i} , sp^{λ_j} (with hybridization parameters λ_i , λ_j) to atoms i, j] and bond angle θ_{ij} is given by Coulson's (1958) directionality theorem (Weinhold and Landis, 2005, p. 110ff),

$$(4) \quad \cos(\theta_{ij}) = -(\lambda_i \lambda_j)^{-1/2}$$

which should be known to every chemistry student. Each hybrid parameter λ is merely a convenient way of expressing the percentage p-character of the hybrid, viz.

$$(5) \quad \lambda = (\%p)/(\%s)$$

which might vary as shown in Table 2 from 0-100% (or any value in between).

Because only three p orbitals and one s orbital comprise the atomic valence shell, the four valence hybrid λ_i 's must satisfy the conservation law

$$(6a) \sum_{i=1-4} 1/(1 + \lambda_i) = 1 \quad (\text{conserve s-character})$$

or equivalently

$$(6b) \sum_{i=1-4} \lambda_i/(1 + \lambda_i) = 3 \quad (\text{conserve p-character})$$

Each conservation law (6a,b) makes clear that increasing the electronegativity of any ligand (thereby increasing λ_i , according to Bent's rule) must necessarily *reduce* the p-character in other hybrids, and thereby alter the bond angles according to Eq. (4). This is simply how hybridization (orbital mixing) works, with no “squashing” required. The simple hybrid/angle equations (4)-(6) allow one to trump VSEPR theory by predicting not only the *direction* but also the approximate *magnitude* of angular change.

type	λ	%-s	%-p	sp^λ - sp^λ angle
pure s	0	100.0	0.0	(isotropic)
sp	1	50.0	50.0	180.0°
sp ²	2	33.3	66.7	120.0°
sp ³	3	25.0	75.0	109.5°
sp ^{3.5}	3.5	22.2	77.8	106.6°
pure p	∞	0.0	100.0	90.0°

Table 2. Hybridization parameter ($0 \leq \lambda \leq \infty$), percentage s/p-character, and associated bond angle for representative sp^λ hybrids [cf. Eqs. (4)-(6)].

Consider, for example, replacement of methane (CH₄) by substituted CH₃X. According to Bent's rule, the equivalent sp³ hybrids of methane (each with 75% p-character) must then be replaced by *inequivalent* hybrids (with $\lambda_H \neq \lambda_X$, to reflect the inequivalent bonding demands of H and X ligands) subject to the conservation constraint (6b),

$$(7a) \quad 3\lambda_H/(1 + \lambda_H) + \lambda_X/(1 + \lambda_X) = 3$$

which can be solved to give

$$(7b) \quad \lambda_H = 2 + 3/\lambda_X$$

The altered λ_X , λ_H values can then be substituted in Eq. (4) to obtain estimated θ_{HX} and θ_{HH} bond angles. For example, if X is highly electronegative (e.g., X = F), its hybrid acquires *more* than 75% p-character [e.g., $\lambda_F = 3.65$ (78.5% p-character), $\lambda_H = 2.79$ (73.6% p-character) in CH₃F (B3LYP/6-311++G** level, idealized tetrahedral geometry)], and Eq. (4) then gives

$$(8a) \quad \theta_{HF} = \arccos[-1/(\lambda_F\lambda_H)^{1/2}] = 108.3^\circ$$

$$(8b) \quad \theta_{HH} = \arccos[-1/\lambda_H] = 111.0^\circ$$

in sensible agreement with fully optimized values (108.6°, 110.3°, respectively). Approximations of λ_X from electronegativity values (as well as limitations of the resulting numerical estimates) are discussed elsewhere (Weinhold and Landis, 2005, p. 138-151), but one requires only the elementary relationship (4) between bond angle θ_{ij} and hybrid descriptors λ_i , λ_j to see how Bent's rule predicts the direction of angular changes from familiar electronegativity differences.

Replacement of a bond pair by a lone pair is also straightforward if we think of the lone pair as bonding to a “ghost” atom X (least electronegative of all!). In H₂O, for example, we expect the in-plane lone pair to exhibit *reduced* p-character, with correspondingly higher p-character in hydride bonds [e.g., $\lambda_{n(\sigma)} = 0.97$ (49.3% p-character) vs. $\lambda_H = 3.05$ (75.3% p-character)]. The predicted hybridization shifts thereby lead to bond-angle changes corresponding to “increased angular volume” around lone pairs, as suggested (for the wrong reasons) by VSEPR theory.

Indeed, with only slight changes of terminology, we can easily re-phrase the familiar VSEPR examples in more accurate and incisive hybrid language. For example, we should describe lone pairs as “s-rich” or “angularly rounded” (rather than “fat” or “more repulsive”). Of course, the temptation to envision rabbit-ear lone pairs should never arise in the reformulated presentation, because the out-of-plane $n_o^{(\pi)}$ lone pair (pure-p, with $\lambda_{n(\pi)} = \infty$) is always excluded from the Bent's rule competition for in-plane p-character.

Why does Bent's rule work? Electrons of a free carbon atom will naturally prefer to remain in a low-energy s-orbital rather than high-energy p-orbital. Chemical C-X bonding can force s-p mixing (hybridization) to lower the overall energy, but the optimal s/p-composition of the C hybrid will naturally depend of how “close” the electron pair remains to the carbon atom. If X is relatively *electropositive*, so that the C-X bond is highly polarized *toward* C, the optimal C hybrid incorporates *increasing s-character* (and increasingly broad angular “roundness”) to minimize the energy. However, if X is electronegative, so that C-X polarization takes the electron pair *away from* C, the optimal C hybrid incorporates *increasing p-character* (and increasingly narrow angular directionality). Bent's rule can also be appropriately re-formulated for

transition metal species (Weinhold and Landis, 2005, p. 421ff), where it continues to provide excellent guidance to molecular structure predictions for mononuclear and polynuclear metallic species. In contrast, VSEPR theory exhibits numerous *spectacular* failures in this domain (Weinhold and Landis, 2005, pp. 389-390, 400, 402, 428, 433, 449, 454, 574).

The hybridization changes implied by Bent's rule can also be recognized in "Walsh diagrams" (Walsh, 1953) that exhibit MO (or NBO) orbital energy as a function of bond angle or other variable of interest. Figure 8 displays the NBO-based Walsh diagrams for bond (σ_{OH}) and lone pair ($n_{\text{O}}^{(\sigma)}$, $n_{\text{O}}^{(\pi)}$) orbitals as p-character reallocates during HOH bond-bending. As shown in Fig. 8, the energy of the in-plane $n_{\text{O}}^{(\sigma)}$ lone pair steadily decreases at smaller HOH bond angles, reflecting its diminished p-character as required by the increased p-character (and higher orbital energy) for the two σ_{OH} bonds. In contrast, the out-of-plane $n_{\text{O}}^{(\pi)}$ is scarcely affected by angular deformations, testifying to its profound inequivalence to $n_{\text{O}}^{(\sigma)}$ with respect to the competition for p-character. Although other factors (including nuclear-nuclear repulsion and Coulomb/exchange variations) contribute to ΔE_{tot} , the dominant orbital-energy dependence is clearly exhibited by the $\epsilon(n_{\text{O}}^{(\sigma)})$ and $\epsilon(\sigma_{\text{OH}})$ NBO variations in Fig. 8, as anticipated by Bent's rule.

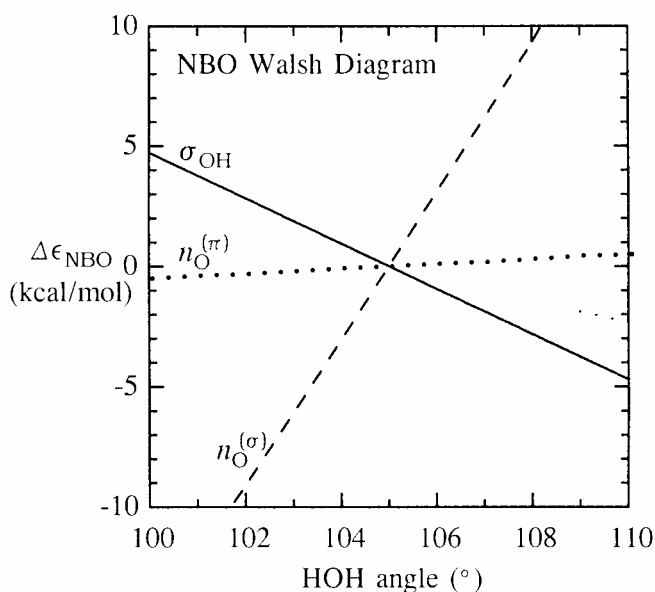


Figure 8. NBO-based Walsh diagram (B3LYP/6-311++G** level), showing NBO orbital energies for σ_{OH} bond (solid line), $n_{\text{O}}^{(\sigma)}$ lone pair (dashed line), and $n_{\text{O}}^{(\pi)}$ lone pair (heavy dotted line) as function of HOH bond angle, reflecting competing in-plane demands for p-character in accordance with Bent's rule.

How can one more accurately characterize the “steric” properties of lone pairs?

Physicist Victor F. Weisskopf (1975) first proposed a visually and mathematically effective formulation of steric repulsion as “kinetic energy pressure.” Steric space-filling or “hardness” properties are generally understood to originate in the Pauli exclusion principle, which limits the maximum occupancy of any spatial orbital to *two* electrons of opposite spin. Equivalently, this principle prevents electron pairs from crowding into the same spatial region, because their orbitals cannot maintain mutual *orthogonality* without incurring additional oscillatory “ripple patterns” (nodal features) that increase the 2nd-derivative “curvature,” and thus the kinetic energy of the orbital. Attempted compression of filled orbitals must therefore result in increasingly severe ripple-like nodal features in the outer overlap region, analogous to the inner nodal features that maintain orthogonality to core electrons of the same symmetry. In each case, the increase in kinetic energy associated with such ripples acts as an opposing “pressure” to resist further compression.⁴

Weisskopf's picture forms the basis of *natural steric analysis* (Badenhoop and Weinhold, 1997a), a standard option of the NBO program (<http://nbo6.chem.wisc.edu>) that quantifies total “steric exchange energy” (E_{NSX}) as well as the pairwise contributions from distinct electron pairs. The R -dependent variations of E_{NSX} provide an excellent approximation for the rare-gas interaction potentials that are considered the prototype of steric exchange effects. The $\Delta E_{\text{NSX}}(R)$ variations are also found to satisfy numerous consistency checks with empirical van der Waals radii and other physical criteria of steric size (Badenhoop and Weinhold, 1997b, 1999). We may therefore employ NBO steric analysis to directly assess the steric-exchange effects with respect to HOH bond-angle variations, as plotted in Figure 9. The figure shows that increasing the HOH angle always causes the overall E_{NSX} steric repulsions to *decrease*, contrary to the lone pair “squashing” that would be expected in VSEPR theory. Various levels of HF or DFT theory differ slightly in overall slope and

⁴ *Why* orbitals must remain mutually orthogonal, and why the curvature of orbital ripple patterns determines kinetic energy, goes back to deep quantum mechanical principles. However, the idea (as epitomized, e.g., in the Bohr relationship $E = h\nu$) that increased number of oscillatory nodes corresponds to unfavorable increase in energy should be familiar to all students. Chemistry students learn the value of using the visual overlap of idealized free-atom orbitals to estimate orbital interaction strength. However, one should recognize that pre-NBOs and other such “visualization orbitals” are merely a convenient mnemonic, whereas the physical solutions of Schrödinger-type eigenvalue equations, as well as the associated perturbation theory equations, are *always* mutually orthogonal (Weinhold, 2003), consistent with Weisskopf's formulation of the steric concept.

individual orbital contributions, but *no* reasonable theoretical level provides support for “VSEPR sterics” as presented in current chemistry textbooks.

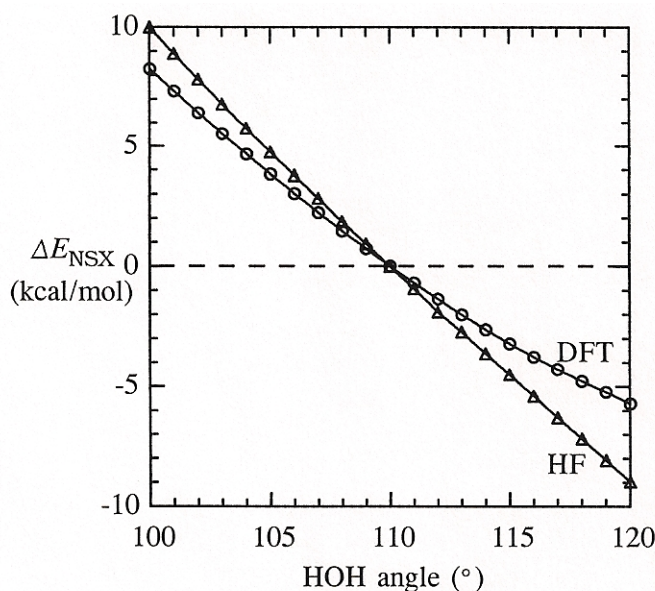


Figure 9. Natural steric-exchange energy variations (ΔE_{NSX}) with H_2O bond angle (referenced to 110°), showing the uniform decrease of steric repulsion toward smaller HOH angles, contrary to expectations of VSEPR theory. Similar trends are found for HF/STO-3G (triangles) and B3LYP/6-311++G** (circles) levels of theory.

An even simpler way to assess relative lone-pair vs. bond-pair “steric size” is by plotting realistic $n_{\text{O}}^{(\sigma)}$, σ_{OH} orbital shapes. (Recall that the orthogonal $n_{\text{O}}^{(\pi)}$ lone pair makes no contribution to sterics in the molecular plane.) Bader *et al.* (1967) proposed the outermost contour value 0.0316 a.u. as closely approximating the effective van der Waals boundary inferred from crystallographic data. With this contour value, Figure 10 compares the apparent orbital sizes for lone-pair vs. bond-pair NBOs in 1-d orbital amplitude (left) and 2-d contour (right) plots for water.

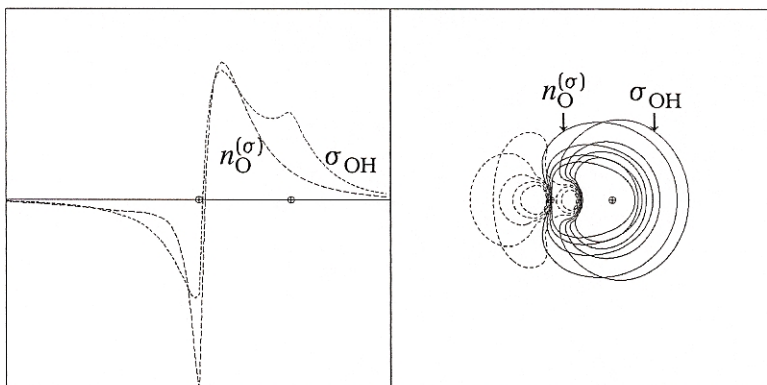


Figure 10. Apparent “steric size” of lone pair ($n_{\text{O}}^{(\sigma)}$) vs. bond pair (σ_{OH}) NBOs of H_2O (B3LYP/6-311++G** level), compared in terms of 1-d orbital amplitude profiles (left) or 2-d contours (right).

As shown in these plots, one can visually judge that the lone pair appears everywhere “sterically hidden” or “inside” the bond pair within a broad cone of approach angles along the forward direction. Neglecting a short-range feature on the $n_{\text{O}}^{(\sigma)}$ backside (seldom the approach direction of chemical interest!), the $n_{\text{O}}^{(\sigma)}$ orbital appears sterically “visible” only in a narrow (near-transverse) angular sector near the nucleus, where its “more rounded” shape is in accordance with Bent's rule. Such simple visual comparison may have greater pedagogical impact than the ΔE_{NSX} evaluations of Fig. 9 in establishing that superficial VSEPR-inspired steric concepts bear little or no relationship to the actual shapes and sizes of lone pair and bonding orbitals as found in modern wavefunctions.

How can the present freshman curriculum be modified to achieve VSEPR-free concepts of directed valency and molecular shape?

A VSEPR-free introduction to hybridization and molecular shapes can be achieved with some shifts of emphasis in standard textbook presentations. As a specific pedagogical model, we consider the textbook “Chemistry: The Molecular Science” (CMS) of Moore *et al.* (2015), where Chapters 5-7 are the respective modules on atoms (CMS-5), diatomic covalent bonding (CMS-6), and polyatomic molecular shape (CMS-7). The overall aim is to retain proper focus on the directional nature of covalent bonding and how hybridized bonding concepts are used to visualize the 3-dimensional structures of molecules, small and large. Modern molecular and orbital visualization tools enable students to begin acquiring accurate visual perceptions of orbital shapes and the maximum-overlap principles that govern molecule construction,

1
2
3 long before the underlying details of quantum mechanics and computational
4 technology need to be confronted.
5
6

7 Specifically, the modified CMS-5 module should develop the concept of atomic
8 orbitals (AOs) and *phase*, using a variety of dot-density and surface diagrams to
9 convey radial and angular features of hydrogenic ground and excited-state atomic
10 orbitals, including the oscillatory sign variations that are needed to keep s, p, d
11 orbitals properly independent (orthogonal) as distinct excitation states. The CMS-6
12 module should similarly develop the *superposition* concept -- the in-phase
13 (constructive) and out-of-phase (destructive) mixing of hydrogenic 1s AOs to form
14 the ground state “bonding” and excited state “antibonding” orbitals of diatomic
15 species such as H_2^+ , H_2 , He_2^+ , and He_2 . (The restricted palette of choices allowed by
16 the Pauli principle should also be emphasized at this point, progressively quenching
17 opportunity for chemical bonding as one moves from H_2 to He_2^+ to He_2). Students are
18 thereby visually introduced to an important special case of the superposition principle:
19 If an electron is offered a choice of localizing on one H atom *or* the other, quantum
20 superposition guarantees that a *better* (in-phase, “bonding”) orbital can be found that
21 involves *sharing* between atoms and *lowering* of energy, the essence of chemical
22 bond formation (Weinhold, 1999).
23
24
25
26
27
28
29

30 The stage is then set for CMS-7, the introduction to polyatomic molecular
31 structure. This module might begin with free-form “student discovery” of gas-phase
32 covalent molecule structures with a tool such as *Models 360*
33 (<http://www.chemeddl.org/resources/models360/models.php?pubchem-11638>), which
34 allows students to visually explore bond lengths, angles, and characteristic “shapes”
35 around divalent, trivalent, or tetravalent atoms in an impressionistic manner. Such
36 explorations can be designed for group work by assigning each member a particular
37 atom and the task of tabulating and seeking generalizations about favored molecular
38 bond lengths (sums of “atomic radii”?) and angles (near-trigonal or tetrahedral?),
39 particularly the propensity to form distinctive shapes in one, two, or three dimensions.
40
41
42
43

44 With such empirical generalizations in hand, one can move to considering bonding
45 of covalent hydrides in 2nd-row elements. Begin with HF, where the valence-shell
46 building blocks of F are 2s, 2p, the former isotropic (undirected) and smaller in size,
47 but lower in energy. If the hydrogen nucleus is located along the z axis, one can see
48 by inspection that only the 2s and 2p_z orbitals of F can have constructive bonding
49 overlap with the 1s of H, whereas the remaining 2p_x and 2p_y orbitals (perpendicular to
50 the bonding axis) must become off-axis “left-overs” for non-bonding (lone pair)
51 electrons. With respect to the apparent alternatives available to on-axis (“active”) 2s,
52 2p_z bonding atomic orbitals of F, the quantum superposition principle once again
53 guarantees that some *mixture* (hybrid) of 2s, 2p_z must give better overlap (and lower
54 energy) than either “pure” alternative alone. As students can readily verify with
55 graphical visualization tools, a 50:50 mixture (2s + 2p_z, “sp hybrid”) gives greater
56
57
58
59
60

1
2
3 directionality and overlap with the target 1s orbital on H than either 2s or 2p_z alone.
4 Such an in-phase sp-hybrid is therefore used to form the 2-center (σ_{FH}) orbital for the
5 bond pair, whereas the out-of-phase sp hybrid (oppositely directed along the z axis)
6 and the unhybridized off-axis 2p_x, 2p_y orbitals contain the lone pairs of the formal
7 Lewis structure. The on-axis sp-hybrid lone pair (with 50% s-character) is naturally
8 quite distinct in energy and shape from the higher-energy off-axis 2p_x, 2p_y lone pairs,
9 discouraging any temptation to think of equivalent (“tripod-like”) spatial distributions
10 and chemical properties of fluoride lone pairs.
11
12
13
14

15 This brings us to the case of water, where the O atom has the usual 2s, 2p_x, 2p_y, 2p_z
16 valence orbitals and each H has the 1s orbital. As in HF, the first OH bond may be
17 oriented along the z axis, using the in-phase (s+p_z) hybrid. Will the second OH bond
18 prefer a linear or bent geometry? If linear, the only option is to use the oppositely
19 directed (s-p_z) hybrid for the second bond pair, which leaves the remaining 2p_x, 2p_y
20 orbitals for lone pairs. If bent (say, in the y-z plane of bonding), an additional 2p_y
21 orbital becomes available to participate in hybridization and bonding (e.g., by forming
22 three equivalent “sp²” hybrids, each of 33% s-character, oriented at 120° to one
23 another) while leaving 2p_x as the p-type lone pair perpendicular to the bonding plane.
24 At this point one can introduce Coulson’s directionality theorem, to determine inter-
25 hybrid angles for various proposed hybrid compositions, and Bent’s rule, to allocate
26 %-s vs. %-p character most sensibly between bonding vs. non-bonding hybrids (or
27 bonding partners of higher vs. lower electronegativity). The elements for discussion
28 of general “sp^λ” hybridization (where λ is the ratio of %-p to %-s character) are
29 thereby in place, and the elementary orbital reasoning underlying both Bent’s rule and
30 the Coulson formula (4) will be seen as highly intuitive and fully consistent with
31 accurate orbital visualizations. One thereby achieves the desired goal of instilling
32 more accurate conceptions of orbitals (automatically consistent with graphical
33 displays of accurate wavefunction properties) and the deep relationships between
34 electronegativity differences, hybrid composition, and molecular geometry, while
35 avoiding superficial VSEPR/rabbit-ears conceptions of water lone pairs.
36
37
38
39
40
41
42
43
44

45 As a pedagogical bonus, one also has the corresponding compositions and shapes
46 of the *antibonding* (unoccupied “non-Lewis”) partners of the final bonding orbitals,
47 which serve as sites of potential *change* of electronic configuration. Thus, students
48 are immediately prepared to focus on the “donors” (occupied Lewis-type orbitals) and
49 “acceptors” (vacant non-Lewis orbitals) that lead to important donor-acceptor
50 interactions (resonance corrections to the elementary Lewis structure picture) or the
51 full electron *transfers* of electronic spectroscopy or chemical reaction phenomena.
52 Appendix 2 includes a current handout for a main-line freshman chemistry course
53 (Chem 104 at the University of Wisconsin, Madison) that illustrates the power of such
54 “donor-acceptor thinking” in perceiving the deep relationships between molecular
55 structure and reactivity at a surprisingly sophisticated level.
56
57
58
59
60

Conclusion

The foregoing examples serve to illustrate how *qualitative* chemical misrepresentations are inspired by VSEPR concepts, and why the teaching of such concepts ought to be sharply downgraded or abandoned. Fairly simple changes in emphasis and language allow one to retain the popular molecular structural predictions of the “VSEPR module,” but to integrate (and extend!) these predictions in the framework of more accurate teaching of hybridization and Bent's rule concepts. The latter form the basis for modern valency and bonding principles that extend successfully to main-group and transition-group species far beyond the scope of freshman chemistry. These principles are also completely consistent with (indeed, derived from and inspired by) the best available computational evidence from modern wavefunctions. They are also consistent with “bottom-up” and “active learning” strategies (Levy Nahum *et al.*, 2008), (Alberts, 2013) to better integrate the problem-solving tools and techniques of modern research into the undergraduate curriculum, and they connect with other recent work (Hinze *et al.*, 2013) on the effectiveness of scientific visualization tools. Pedagogical eradication of VSEPR/rabbit-ear trappings is thus a win-win situation, both for the freshman-level course as well as the advanced courses that aim to bring students toward the frontiers of current chemical research.

References

- Alberts, B. (2013), Prioritizing science education, *Science*, **340**, 249.
- Anet, F.A.L. and Yavari, I. (1977), Nitrogen inversion in piperidine, *J. Am. Chem. Soc.* **99**, 2794-2796.
- Anslyn, E. V. and Dougherty, D. (2006), *Modern Physical Organic Chemistry*, University Science Books: Sausalito, CA, p. 102ff.
- Badenhoop, J. and Weinhold, F. (1997a), Natural bond orbital analysis of steric interactions *J. Chem. Phys.* **107**, 5406-5421.
- Badenhoop, J. and Weinhold, F. (1997b), Natural steric analysis: Ab initio van der Waals radii of atoms and ions *J. Chem. Phys.* **107**, 5422-5432.
- Badenhoop, J. and Weinhold, F. (1999), Natural steric analysis of internal rotation barriers, *Int. J. Quantum Chem.* **72**, 269-280.
- Bader, R. F. W., Henneker, W. H. and Cade, P. E. (1967), Molecular charge distributions and chemical binding *J. Chem. Phys.* **46**, 3341-3363.
- Beagley, B., Eckersley, G. H., Brown, D. P. and Tomlinson, D. (1969), Molecular structure of S₂Cl₂, *Trans. Faraday Soc.* **65**, 2300-2307.

- 1
2
3
4 Beagley, B. and McAloon, K. T. (1971), Electron-diffraction study of the molecular
5 structure of dimethyldisulphide, $(\text{CH}_3)_2\text{S}_2$, *Trans. Faraday Soc.* **67**, 3216-3222.
6
- 7 Bent, H. A. (1961), An appraisal of valence-bond structures and hybridization in
8 compounds of the first-row elements, *Chem. Rev.* **61**, 275-311.
9
- 10
11 Bickelhaupt, F. M. and Baerends. E. J. (2003), The case for steric repulsions causing
12 the staggered conformation of ethane, *Angew. Chem. Int. Ed.* **42**, 4183-4188.
13
- 14
15 Carpenter, J.E. and Weinhold, F. (1988), Torsion-vibration interactions in hydrogen
16 peroxide. 2. Natural bond orbital analysis, *J. Chem. Phys.* **92**, 4306-4313.
17
- 18
19 Clauss, A. D. and Nelsen, S. F. (2009), Integrating computational molecular modeling
20 into the undergraduate organic chemistry curriculum, *J. Chem. Educ.* **86**, 955-958.
21
- 22
23 Coulson, C. A. (1952), *Valence*, 2nd ed., Oxford: London, Chapter 8.
24
- 25
26 Delongchamps, P. (1983), *Stereoelectronic Effects in Organic Chemistry*, Pergamon:
27 Oxford.
28
- 29
30 Fock, V. (1930), Approximation methods for solution of the quantum mechanical
31 many-body problem (*in German*), *Z. Physik* **61**, 126-148.
32
- 33
34 Foresman, J. B. and Frisch, A (1996), *Exploring Chemistry with Electronic Structure*
35 *Methods*, 2nd ed., Gaussian, Inc.: Pittsburgh.
36
- 37
38 Gillespie, R. J. and Nyholm, R. S. (1957), Inorganic stereochemistry, *Quart. Rev.*
39 (*London*) **11**, 339-380.
40
- 41
42 Gillespie, R. J. (1963), The valence-shell electron-pair repulsion (VSEPR) theory of
43 directed valency, *J. Chem. Educ.* **40**, 295-301.
44
- 45
46 Gillespie, R. J. (1974), A defense of the valence shell electron pair repulsion (VSEPR)
47 model, *J. Chem. Educ.* **51**, 367-370.
48
- 49
50 Gillespie, R. J. (2004), Teaching molecular geometry with the VSEPR model, *J.*
51 *Chem. Educ.* **81**, 298-304.
52
- 53
54 Hahn, J., Schmidt, P., Reinartz, K., Behrend, J., Winnewisser, G. and Yamada, K. M.
55 T. (1991), Synthesis and molecular structure of disulfane, *Z. Naturforsch.* **46b**, 1338-
56 1342.
57
58
59
60

1
2
3
4
5
6
7
8
9
10
11
12
13
14
15
16
17
18
19
20
21
22
23
24
25
26
27
28
29
30
31
32
33
34
35
36
37
38
39
40
41
42
43
44
45
46
47
48
49
50
51
52
53
54
55
56
57
58
59
60

Hinze, S. R., Rapp, D. N., Williamson, V. M., Shultz, M. J. Deslongchamps, G. and Williamson, K. C. (2013), Beyond ball-and-stick: Students' processing of novel STEM visualizations. *Learning and Instruction* **26**, 12-21.

Jones, R. A. Y., Katrizky, A. R., Saba, S. and Sparrow, A. J. (1974), The conformational analysis of saturated heterocycles. Part LXIII. Tetrahydro-1,2 oxazines and related acyclic hydroxylamines, *J. Chem. Soc., Perkin Trans. 2*, 1554-1557.

Jorgensen, W. L. and Salem, L. (1973), *The Organic Chemist's Book of Orbitals*, Academic: New York, p. 42.

Katrizky, A. R. and Lagowski, J. M. (1967), *Principles of Heterocyclic Chemistry*, Menthuen: London, p. 144ff.

Kirby, A.J. (1983), *The Anomeric Effect and Related Stereoelectronic Effects at Oxygen*, Springer: New York.

Kniep, R., Korte, L. and Mootz, D. (1983), Crystal Structures of Compounds A_2X_2 ($A = S, Se, X = Cl, Br$) (*in German*), *Z. Naturforsch.* **38b**, 1-6.

Kuczkowski, R. L. (1964), The mass and microwave spectra, structures, and dipole moments of the isomers of sulfur monofluoride, *J. Am. Chem. Soc.* **86**, 3617-3621.

Laing, M. (1987), No rabbit ears on water. The structure of the water molecule: What should we tell the students?, *J. Chem. Educ.* **64**, 124-129.

Levy Nahum, T., Mamlok-Naaman, R, Hofstein, A. and Kronik, L. (2008), A new "bottom-up" framework for teaching chemical bonding, *J. Chem. Educ.* **85**, 1680-1685.

Marsden, C. J., Oberhammer, H., Lösing, O. and Willner, H. (1989), The geometric structures of the disulphur difluoride isomers: an experimental and ab initio study, *J. Mol. Struct.* **193**, 233-245.

Moore, J. W., Stanitski, C. L. and Jurs, P. C. (2015), *Chemistry: The Molecular Science*, 5th ed., Cengage Learning, Stamford, CT.

Nelsen, S. F., Thompson-Colon, J. A., Kirste, B., Rosenhouse, A. and Kaftory, M. (1987), One-electron oxidation of 3-substituted 2-oxa-3-azabicyclo[2,2,2]octane derivatives, *J. Am. Chem. Soc.* **109**, 7128-7136.

1
2
3 Pauling, L. (1931), The nature of the chemical bond. Application of results obtained
4 from the quantum mechanics and from a theory of paramagnetic susceptibility to the
5 structure of molecules. *J. Am. Chem. Soc.* **53**, 1367-1400.
6
7

8 Petillo, P. A. and Lerner, L.E. (1993), Origin and quantitative modeling of anomeric
9 effect, in Thatcher, G. R. J. (ed.), *The Anomeric Effect and Related Stereoelectronic*
10 *Effects*, American Chemical Society: Washington, Chapter 9.
11
12

13 Pophristic, V. and Goodman, L. (2001), Hyperconjugation not steric repulsion leads to
14 the staggered structure of ethane. *Nature* **411**, 565-568.
15
16

17 Reed, A. E. and Weinhold, F. (1985), Natural localized molecular orbitals, *J. Chem.*
18 *Phys.* **83**, 1736-1740.
19
20

21 Riddell, F. G. (1981), The conformations of hydroxylamine derivatives. *Tetrahedron*
22 **37**, 849-858.
23
24

25 Schreiner, P. R. (2002), Teaching the right reasons: Lessons from the mistaken origin
26 of the rotational barrier in ethane, *Angew. Chem. Int. Ed.* **41**, 3579-3582.
27
28

29 Shaik, S. and Hiberty, P. C. (2008), *A Chemist's Guide to Valence Bond Theory*
30 Wiley-Interscience: Hoboken, NJ.
31
32

33 Slater, J. C. (1931), Directed valence in polyatomic molecules. *Phys. Rev.* **37**, 481-
34 489.
35
36

37 Steudel, R. (1975), Properties of sulfur-sulfur bonds, *Angew. Chem. Int. Ed.* **14**, 655-
38 664.
39
40

41 Streitwieser, A., Jr. (1961), *Molecular Orbital Theory for Organic Chemists*, Wiley:
42 New York.
43
44

45 Sutter, D., Dreizler, H. and Rudolph, H. D. (1965), Microwave spectrum, structure,
46 dipole moment, and rotation barrier potential of dimethyldisulfide (*in German*), *Z.*
47 *Naturforsch.* **20a**, 1676-1681.
48
49

50 Walsh, A. D. (1953), The electronic orbitals, shapes, and spectra of polyatomic
51 molecules, *J. Chem. Soc. London* **1953**, 2260-2331.
52
53

54 Weinhold, F. (1999), Chemical bonding as a superposition phenomenon, *J. Chem.*
55 *Educ.* **1999**, 76, 1141-1146.
56
57

58 Weinhold, F. (2003), Rebuttal to the Bickelhaupt-Baerends case for steric repulsion
59 causing the staggered conformation of ethane, *Angew. Chem. Int. Ed.* **42**, 4188-4194.
60

1
2
3 Weinhold, F. (2012), Natural bond orbital analysis: A critical overview of its
4 relationship to alternative bonding perspectives, *J. Comp. Chem.* **33**, 2363-2379.
5
6

7 Weinhold, F. and Klein, R. A. (2014), What is a hydrogen bond? Resonance
8 covalency in the supramolecular domain, *Chem. Educ. Res. Pract.* (doi:
9 10.1039/C4RP00030G).
10
11

12 Weinhold, F. and Landis, C. R. (2001), Natural bond orbitals and extensions of
13 localized bonding concepts, *Chem. Educ. Res. Pract.* **2**, 91-104.
14
15

16 Weinhold, F. and Landis, C. R. (2005), *Valency and Bonding*, Cambridge U. Press:
17 London.
18
19

20 Weinhold, F. and Landis, C. R. (2012), *Discovering Chemistry with Natural Bond*
21 *Orbitals*, Wiley: Hoboken NJ.
22
23

24 Weisskopf, V. W. (1975), Of atoms, mountains, and stars: a study in qualitative
25 physics, *Science* **187**, 605-612.
26
27

28 Winnewisser, G., Winnewisser, M. and Gordy, P.J. (1968), Millimeter-wave
29 rotational spectrum of HSSH and DSSD. 1. Q branches, *J. Chem. Phys.* **49**, 3465-
30 3478.
31
32

33 Yokozeki, A. and Bauer, S. H. (1976), Structures of dimethyl disulfide and methyl
34 ethyl disulfide, determined by gas-phase electron diffraction. A vibrational analysis
35 for mean square amplitudes, *J. Phys. Chem.* **80**, 618-625.
36
37

38 Zimmerman, H. E. (1963), A new approach to mechanistic organic photochemistry, in
39 Noyes, W.A. Jr., Hammond, G.S. and Pitts, J.N. Jr. (eds.), *Advances in*
40 *Photochemistry*, Interscience: New York, Vol. 1, p. 183-208.
41
42
43
44
45
46
47
48
49
50
51
52
53
54
55
56
57
58
59
60

Appendix 1: Critique of the purported “unitary equivalence” of conflicting lone pair depictions

A version of the unitary invariance argument for inequivalent and equivalent lone pairs is presented in the recent monograph of Shaik and Hiberty (2008, pp. 107-109) which may be taken as representative. In this argument, equivalent rabbit-ear hybrids h_r , $h_{r'}$ are expressed (in unnormalized form) by proportionality relations of the form

$$(A-1a) \quad h_r \propto n + \lambda p$$

$$(A-1b) \quad h_{r'} \propto n - \lambda p$$

where $p = p_y$ (perpendicular to the molecular plane), n is an in-plane sp^n -type hybrid, and λ is a mixing parameter (left unspecified in their discussion). Visually (cf. Scheme 5.3 of the Shaik-Hiberty discussion), such mixtures suggest a superficial resemblance to sp^3 hybrids. However, only $\lambda = 1$ is allowed by Fock's theorem, because the transformation is otherwise non-unitary and h_r , $h_{r'}$ become nonorthogonal. The envisioned orthonormal rabbit-ears hybrids must therefore be expressed more explicitly as

$$(A-2a) \quad h_r = 2^{-1/2}(n + p)$$

$$(A-2b) \quad h_{r'} = 2^{-1/2}(n - p)$$

with associated orbital energies

$$(A-3a) \quad \varepsilon_r = (\varepsilon_n + \varepsilon_p + 2F_{np})/2$$

$$(A-3b) \quad \varepsilon_{r'} = (\varepsilon_n + \varepsilon_p - 2F_{np})/2$$

These orbitals are indeed equivalent ($\varepsilon_r = \varepsilon_{r'}$), because off-diagonal $F_{n,p} = \langle n|F|p \rangle$ matrix elements between MOs are vanishing.

However, the transformed orbitals h_r , $h_{r'}$ are generally not “ sp^3 hybrids” and must exhibit rather strange energetic interactions. If we assume, e.g., that n is an sp^2 hybrid along the z axis

$$(A-4) \quad n = 3^{-1/2}(s + 2^{1/2}p_z)$$

then h_r , $h_{r'}$ become explicitly

$$(A-5a) \quad h_r = 6^{-1/2}[s + 3^{1/2}p_y + 2^{1/2}p_z]$$

$$(A-5b) \quad h_{r'} = 6^{-1/2}[s - 3^{1/2}p_y + 2^{1/2}p_z]$$

neither of which (83% p-character) is of idealized sp^3 form. Moreover, these orbitals have the surprising Fock matrix interaction element

$$(A-6) \quad F_{r,r'} = \langle h_r | F | h_{r'} \rangle = 1/2 \langle n + p | F | n - p \rangle = (\epsilon_n - \epsilon_p)/2$$

even though $\langle h_r | h_{r'} \rangle = 0$! For water (B3LYP/6-311++G** level), this interaction evaluates to an alarmingly large value

$$(A-7) \quad F_{r,r'} = -108 \text{ kcal/mol}$$

which could not be considered “ignorable” except in the context of a crude Hückel-like model (with the assumption $F_{r,r'} = k \langle h_r | h_{r'} \rangle = 0$, *perforce* vanishing). In this limit, the lone pairs must also be implicitly assumed to be degenerate in energy ($\epsilon_n = \epsilon_p$), in conflict with spectroscopic properties such as first recognized by Zimmerman (1963). Thus, the supposed “equivalence” of (n,p) vs. $(h_r, h_{r'})$ lone pairs rests on approximations that are unacceptable by current standards of accuracy.

Appendix 2: A sample freshman-level handout on donor-acceptor interactions

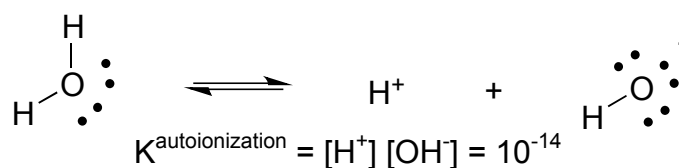
Bonding and Donor-Acceptor Concepts

Chem 104

Prof. Landis

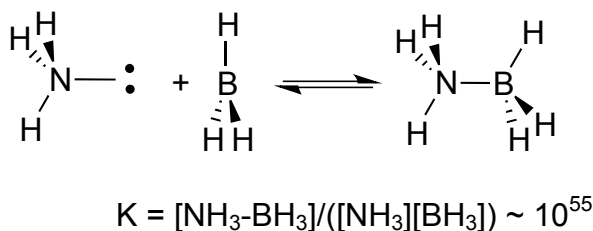
Chemistry presents a bewildering array of transformations: acid-base reactions, doping of semiconductors, transfer of electrons in oxidation and reduction reactions, condensation/hydrolysis pairs, substitution reactions, formation of hydrogen bonds, and so on. Rather than memorizing thousands of reactions it is helpful to think about *how* they occur using the concept of donor-acceptor interactions. This unifying concept provides a deep framework that reveals the underlying kinships amongst seemingly unrelated reactions.

An acceptor is an atom, molecule, ion, or even solid-state material that has vacant orbitals to which electrons can be donated. A donor is an atom, molecule, ion, or material that has loosely held electrons that can be donated to an acceptor. To illustrate the donor/acceptor concept consider the following representation of the autoionization equilibrium of water (N.B., this representation does *not* show the other water molecules that interact with the reactants and products in bulk liquid water).



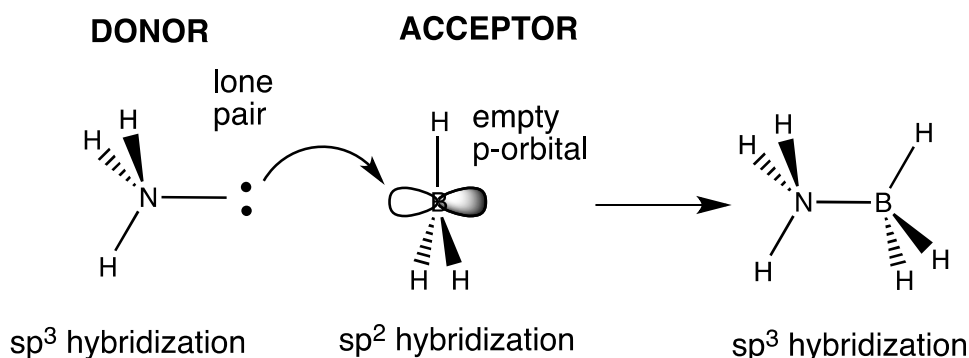
Focus on the *right-to-left (reverse)* reaction direction. The H^+ ion is a hydrogen atom with no electrons in its valence 1s shell – i.e., a bare proton. The presence of an empty valence 1s orbital makes H^+ an electron pair acceptor. The OH^- ion has three lone pairs in its valence shell that can be donated to an empty orbital. From the donor-acceptor perspective, the formation of the O-H bond of water is the result of a strong donor, OH^- , donating an electron pair to a strong acceptor, H^+ , to make an electron-pair covalent bond. The equilibrium lies to the left, as might be expected when a strong donor (OH^-) and acceptor (H^+) are allowed to react.

Consider another example that you may have seen in previous chemistry courses: the reaction of ammonia with borane to make the Lewis acid-base adduct.



The formation of $\text{H}_3\text{N-BH}_3$ from ammonia and borane is very favorable (the equilibrium constant is estimated to be very large), suggesting that ammonia is a good donor and BH_3 is a good acceptor. To better understand the acceptor properties of BH_3 we need to first consider the bonding in BH_3 using a localized bond (aka valence bond) approach.

The B ground state electron configuration is $[\text{He}]2s^22p^1$. Therefore, there are three valence electrons and four valence atomic orbitals, one 2s and the three 2p orbitals, available to make bonds. In BH_3 the three B-H bonds have sp^2 hybridization, meaning that two p-orbitals and one s-orbital were mixed together in making three equivalent sp^2 hybrids. These orbitals all lie in the same plane, yielding a trigonal planar geometry with 120° bond angles. But only *two* of the *three* p-orbitals in the valence shell of B were used to make the B-H bonds. This means that one p-orbital is vacant; it lies perpendicular to the plane of B and H atoms. The vacant p-orbital of B is an electron pair acceptor.



Now look at the Lewis structure for NH_3 . You should be able to devise the following descriptors: approximately sp^3 hybridization of the N atom, three N-H bonds, one lone pair, and a trigonal pyramidal molecular structure. The lone pair is a potential donor. When an ammonia molecule and a borane molecule come close to one another, the lone pair on N can be donated into the empty p-orbital on B to create a donor-acceptor interaction. We symbolize this donor-acceptor interaction with a *curved arrow*. This donor-acceptor interaction increases as the two molecules come closer together, ultimately resulting in a N-B bond. The increase in bond number at B forces the hybridization to change from sp^2 to sp^3 , and the final $\text{H}_3\text{N-BH}_3$ molecule has a tetrahedral arrangement of bonds.

Strengths of Donors and Acceptors

In the previous example we emphasized that *any* lone pair is a potential donor. But not all lone pairs are equally good donors. Engagement in a donor-acceptor interaction requires that the donor electron pair shift from being localized solely on one atom to being shared with the acceptor. This suggests that the *more tightly a donor lone pair is localized on the atom, the poorer its donor ability*. As a result, charge and electronegativity strongly affect the donor strength of a lone pair.

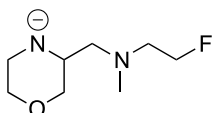
Consider the three examples of functional groups with lone pairs: methylamine, methanol, and fluoromethane. The order of electronegativity is $\text{F} > \text{O} > \text{N}$.

Electronegativity represents the tendency of an atom to draw electrons toward itself when making a bond. In the context of making donor-acceptor bonds, we can expect electronegativity to correlate inversely with the donor ability of a lone pair. In other words, we expect the *lone pair donor strength to increase as N>O>F*.

Charge, also, affects donor ability. Consider a neutral amine (NH_3) and an amide anion (NH_2^-). The anion has an excess of negative charge, making the electron pairs easier to donate than the more tightly held lone pair of the neutral atom. Thus, as the *negative charge of a donor atom increases, the donor strength increases*. Therefore we expect the donor abilities of neutral and anionic N, O, and F lone pairs to exhibit the trend $\text{NH}_2^- > \text{NH}_3$; $\text{OH}^- > \text{OH}_2$; $\text{F}^- > \text{F-H}$.

ConcepTest 78

How many lone pair donor atoms are present in the molecule below?



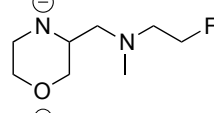
- A. 1 donor
- B. 2 donors
- C. 3 donors
- D. 4 donors
- E. 5 donors

Landis Chem 104 2014 Spring

205

ConcepTest 78 Answer

How many lone pair donor atoms are present in the molecule below?



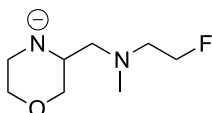
- A. 1 donor
- B. 2 donors
- C. 3 donors
- D. 4 donors ★
- E. 5 donors

Landis Chem 104 2014 Spring

206

ConcepTest 79

Which donor atom is expected to be the strongest donor?



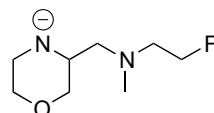
- A. -NR_2
- B. OR_2
- C. NR_3
- D. FR

Landis Chem 104 2014 Spring

1

ConcepTest 79 Answer

Which donor atom is expected to be the strongest donor?



- A. -NR_2 ★ Donor Order
Anionic N > neutral N > O > F
 - B. OR_2
 - C. NR_3
 - D. FR
- Anion > Neutral
Donor Strength decreases with increasing EN

Landis Chem 104 2014 Spring

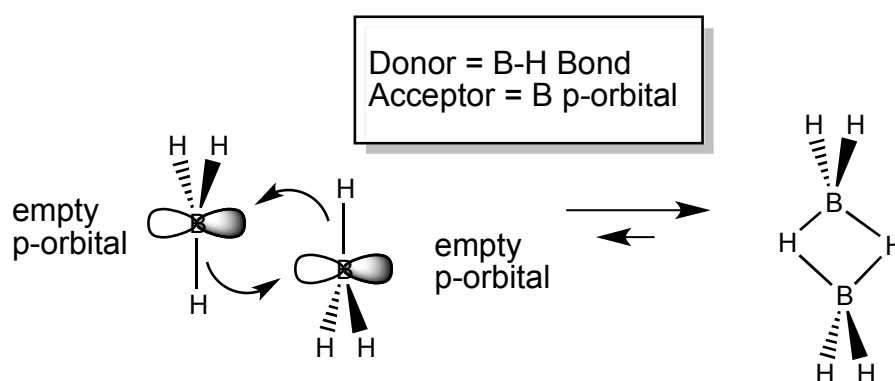
208

We can use similar reasoning to rationalize the relative *acceptor* abilities of atoms with vacant valence orbitals. The molecule BH_3 is isoelectronic with the molecular cation $^+\text{CH}_3$ (called the methyl carbenium ion). Analogously with BH_3 , the methyl cation has a trigonal planar structure with an empty p-orbital lying perpendicular to the molecular plane and three C-H bonds made from C sp^2 hybrid orbitals lying in the plane. However the positive charge of $^+\text{CH}_3$ makes it a much stronger acceptor than neutral BH_3 . As the electron pair of a donor moves closer to the $^+\text{CH}_3$ acceptor, it feels the strong attraction of a positive charge that is absent in the case of neutral BH_3 . Similar reasoning suggests that the more electronegative the acceptor atom, the stronger the acceptor

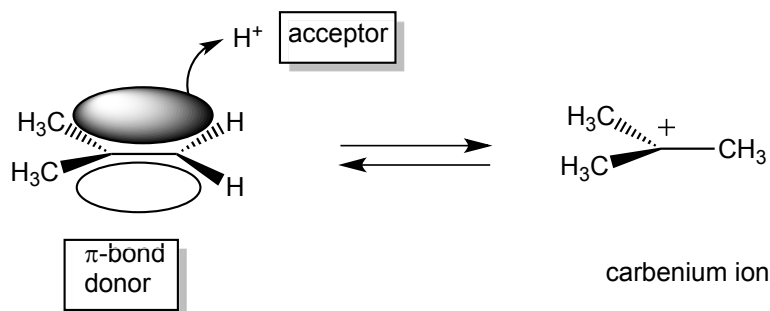
character. Therefore we expect the acceptor strengths to follow trends like: ${}^+\text{CH}_3 > {}^+\text{SiH}_3$ and ${}^+\text{CH}_3 > \text{BH}_3$.

Donors and Acceptors Beyond Lone Pairs and Empty Valence Atomic Orbitals

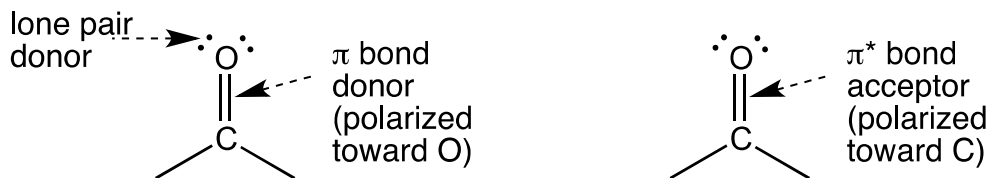
Electron pairs of bonds, also, can engage in donor-acceptor interactions. For example, free BH_3 molecules are rarely observed; instead the dimer, B_2H_6 , is the common form of this compound. As described above, BH_3 is a good acceptor because it has an empty valence p-orbital on boron. When two BH_3 molecules approach one another, the B-H bond pairs can act as donors with B-H pair of each molecule donated into the empty p-orbital of the other. In general, electron pairs in bonds are weaker donors than lone pairs of electrons.



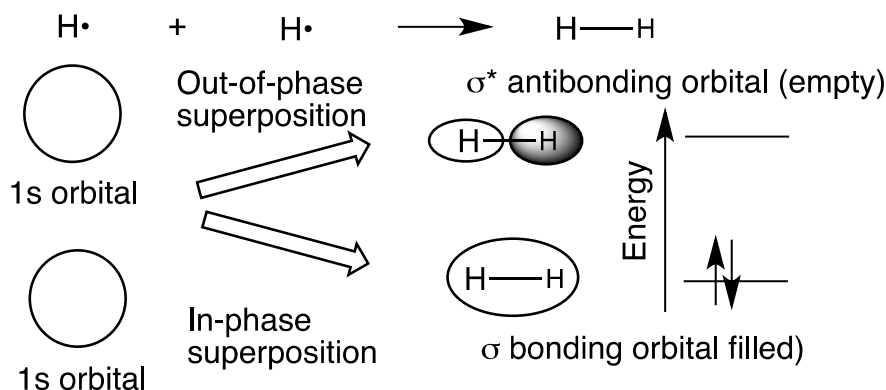
The C-C multiple bonds of unsaturated organic molecules have both σ - and π -bonding electron pairs. The π -bonds are weaker than the σ -bonds, implying that π -bonds are potential donors. A prototypical reaction of this type is the reaction of isobutene with an H^+ to form a carbenium ion. The π -bond is the donor and H^+ is the acceptor. The product carbenium ion is itself a strong acceptor. Therefore, when scanning a molecule for potential donor sites, pay attention to π -bonds also; be on the lookout for alkenes, alkynes, and molecules with C=O bonds (aldehydes, ketones, esters, etc.) or C=N π -bonds (nitriles, imines, etc.). The π -bond, like other bond electron pairs, is not a strong donor in the thermodynamic sense (vide infra) but can be important kinetically.



Molecules with C=O functional groups are called carbonyls. Note that one could consider both the C=O π -bond and the lone pairs on the oxygen atoms as potential donor groups.



Although it may seem strange, antibonding orbitals can serve as electron pair acceptors. Let's first review what we mean by an antibonding orbital. When two singly occupied orbitals, such as the 1s orbitals of two H atoms, come close in space the quantum principle of superposition dictates that two molecular orbitals are formed. One superposition has "in-phase" character and results in accumulation of electron density between the two nuclei. This new orbital is called a *bonding* orbital, because it results in a lower enthalpy of the bonded atoms relative to the separated atoms. The other superposition has "out-of-phase" character and results in a depletion of electron density between the two nuclei. Placing electrons in the "out-of-phase" superposition does NOT lower the enthalpy of the bonded atoms relative to the separate atoms. Therefore, the "out-of-phase" superposition is called an *antibonding* orbital. Antibonding orbitals are designated by a * as in σ^* for a sigma antibond and π^* for a pi antibond.

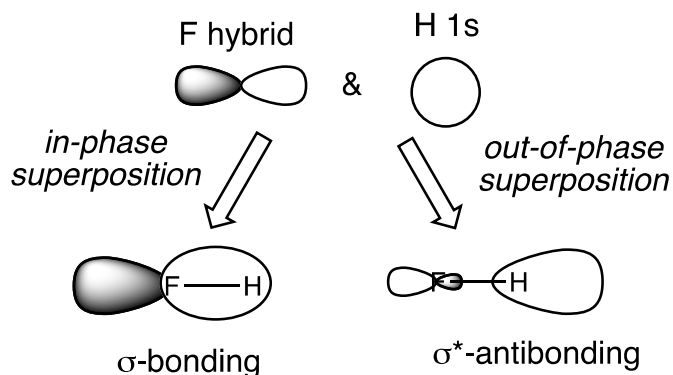


For two atoms that are bonded together, the bonding orbital is filled with a pair of electrons and lies lower in energy than the unfilled antibonding orbital. What you should remember is that every time a filled bonding orbital is created an unfilled antibonding orbital is made: "for every bond, an antibond".

Antibonding orbitals are more than mathematical curiosities. An *antibond is an unfilled orbital that can accept a pair of electrons*. In particular, the antibonding orbitals associated with weak or highly polar bonds are good acceptors. For example, the C-C π bonds of hydrocarbons are weaker than the σ -bonds. Correspondingly, the C-C π^* orbitals are better acceptors than C-C or C-H σ^* orbitals (you can rationalize this by considering relative orbital energies; in a weak bond the bonding orbitals are higher in energy and weak bonds are lower in energy relative to a strong bond).

When a σ - or π -bond is formed between atoms of different electronegativity, such as hydrogen fluoride, the filled bonding orbital is *polarized* toward the more electronegative atom. In other words the electrons are distributed unequally with the more

electronegative atom getting more than its “share”. Accurate quantum mechanical computations reveal the shared electron pair of HF is 80% associated with the F atom and only 20% associated with the H atom – hardly equal sharing.



According to the principle of superposition, if the bonding orbital is polarized toward the more electronegative atom, *the antibonding orbital is polarized toward the less electronegative atom*. In the graphic depiction above, the polarization of the antibonding orbital toward H is shown by the “fatter” H component and the “shrunken” F part. Quantum mechanical calculations show the H-F σ^* antibonding orbital to have 80% contribution from H and 20% from F. Orbital polarization means that donor-acceptor interactions with σ^* or π^* antibonds will be strongest when the donor comes close to the less electronegative atom of the bonded pair. The less electronegative atom will tend to have greater partial positive charge, which also will favor interaction with the incoming donor electrons.

ConcepTest 81

How many potential *acceptor* sites does this molecule have?

A. One
B. Two
C. Three
D. Four
E. Five

Landis Chem 104 2014 Spring 205

ConcepTest 81 Answer

How many potential *acceptor* sites does this molecule have?

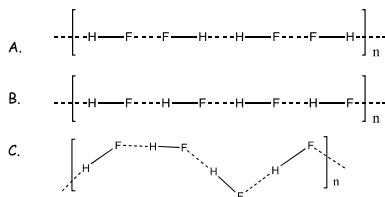
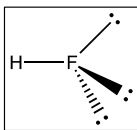
A. One
B. Two
C. Three ★
D. Four
E. Five

Landis Chem 104 2014 Spring 206

Consider a simple example before we go on to more complex reactions: hydrogen bonding in solid HF. Two HF molecules can form a hydrogen bonded “super molecule” or chain through the donation of a F lone pair of one HF molecule into the σ^* orbital of another HF molecule.

ConcepTest 80

Hydrogen bonding in H_nX molecules is the result of strong donor-acceptor interactions between X lone pairs and H-X σ^* antibonds. Based on this description which of the structures below is expected for solid HF?

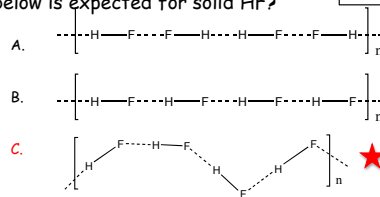
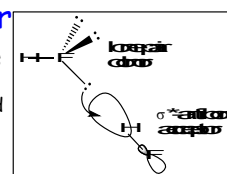


Landis Chem 104 2014 Spring

203

ConcepTest 80 Answer

Hydrogen bonding in H_nX molecules is the result of strong donor-acceptor interactions between X lone pairs and H-X σ^* antibonds. Based on this description which of the structures below is expected for solid HF?



Landis Chem 104 2014 Spring

204

Common Donors

Lone pairs: C, N, O, P, S, Halogens
 π bonds: C=C, C=O, C=N, and C \equiv C
 σ bonds: C-Li, C-Mg, C-Zn, H-B

Common Acceptors

Empty valence orbitals: H⁺, carbenium ions, trivalent B & Al
 π^* orbitals: C=C, C=O, and C=N
 σ^* orbitals: H-Halogen, H-O, H-N, C-halogen, C-O

Whether a strong donor-acceptor interaction will occur depends on **both** the donor and acceptor. In general the C=C π -bond is a modest donor, but H⁺ is a strong acceptor. Therefore, the π -bond-to-H⁺ donor-acceptor interaction can lead to formation of a carbenium ion in at least low equilibrium concentrations. We might not expect a significant donor-acceptor interaction at all for an alkene interacting with a substantially weaker acceptor than H⁺.

For those that go on to take organic chemistry, many instances of reactions that involve reactant donor-acceptor interactions will be seen. We focus here on the acid catalyzed conversion of an alcohol and isobutene to an ether.

Arrows: Curved, Straight, and Double-headed

We need to be very particular about how we use arrows in Chemistry. In Chemistry 104 the following definitions and uses will be followed rigorously.

1) Straight arrows with one arrow-head in either forward or reverse or both directions:



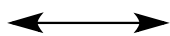
are chemical reaction arrows and indicate the *rearrangement of atom positions and bonds* in going from reactant to products.

2) Curved arrows indicate donor-acceptor interactions of electrons and vacant orbitals

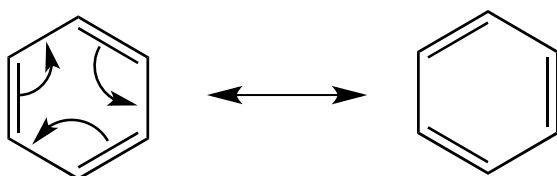


Changes in atom positions are NOT implied by a curved arrow.

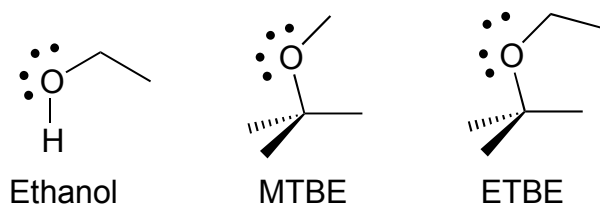
3) A single double-headed arrow represents resonance:



In resonance depictions ALL ATOMS ARE STATIONARY, thus no chemical reaction is occurring. Resonance means that a single Lewis structure is insufficient to describe the distributions of electrons in a molecule. It is valid to use curved arrows to depict the donor-acceptor interactions that transform one Lewis structure into another. For the resonance in benzene the donors are the filled π -orbitals of one double bond and the acceptors are the unfilled π^* orbitals adjacent double bonds.

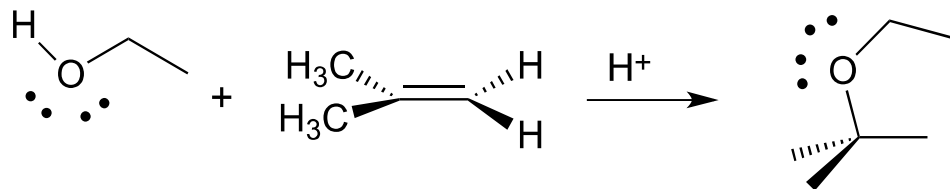


Acid-Catalyzed Synthesis of ETBE from Ethanol and Isobutene

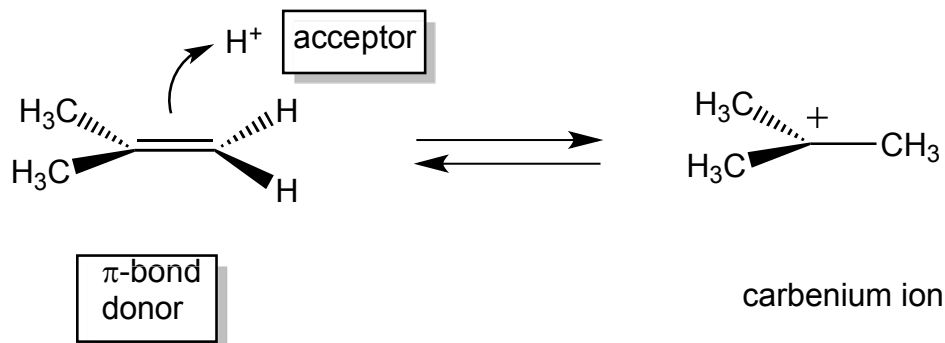


Reformulated gasolines (RFGs) have oxygenated additives such as ethanol, MTBE, and ETBE. Because these molecules already have oxygen incorporated in their structure, they enable car engines to operate with leaner air-to-fuel ratios than with pure hydrocarbon gasoline while achieving high combustion efficiency.

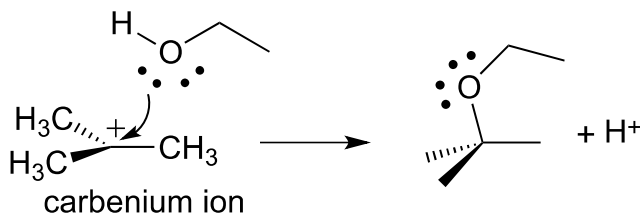
Commercially, ETBE is made by the reaction of ethanol and isobutene (also called 2-methylpropene) in the presence of an acid catalyst. In the absence of a catalyst, this reaction is very slow, too slow to make the quantities needed for reformulated gasoline. Our goal here is to see how the donor-acceptor paradigm provides insight into the nature of acid catalysis of the reaction between isobutene and ethanol.



As we have already seen, the π -bond of an alkene can act as an electron pair donor and H^+ is a good acceptor. This donor-acceptor interaction leads to the formation of a carbenium ion.

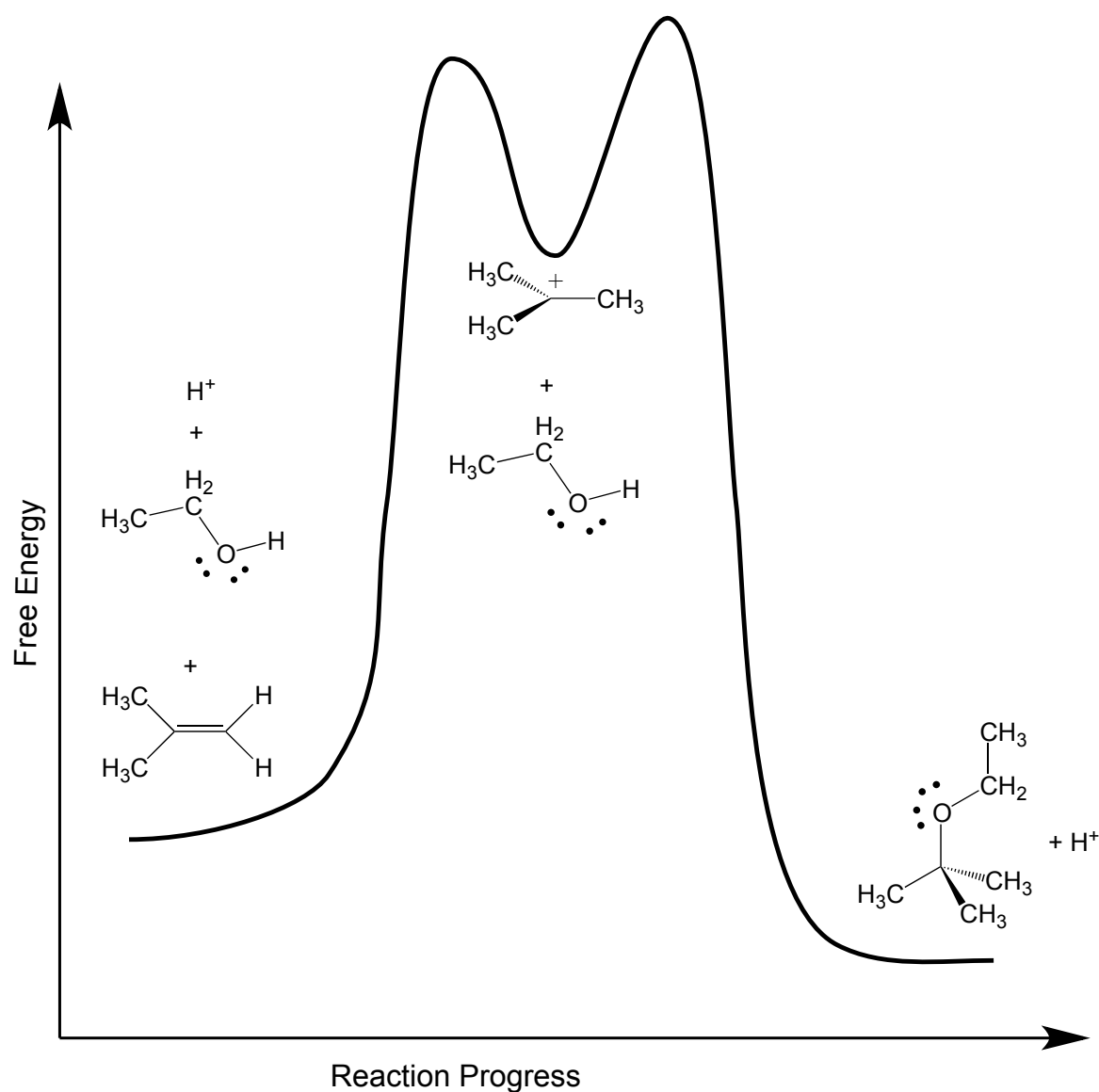


But the carbenium ion itself is a very strong acceptor and the oxygen lone pairs of ethanol are good donors. This suggests a strong donor-acceptor interaction that ultimately leads to the product and regenerates the H^+ catalyst by loss of H^+ from the



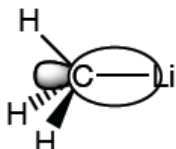
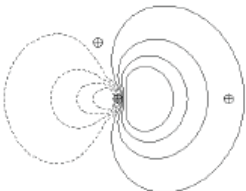
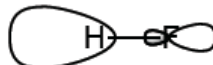
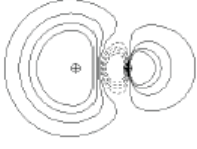
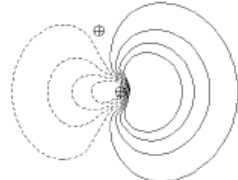
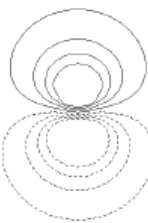
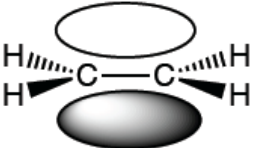
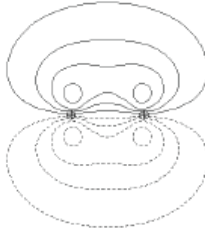
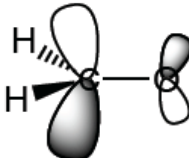
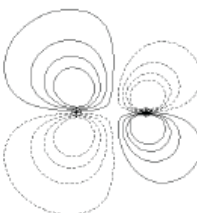
protonated ether oxygen. Remember that, by definition, a catalyst must not be consumed or created in the overall reaction. This does not mean that the catalyst is not involved in bond-making and breaking as the reaction progresses – as we have seen H^+ is intimately involved in reacting with isobutene. Rather, catalysis requires that the reaction of H^+ in the first step must be paired with a step in which the H^+ is regenerated as a reaction product.

Acid-catalyzed formation of an ether from an alcohol and alkene is an example of a two-step reaction in which the carbenium ion is an intermediate. We can depict this overall transformation using a reaction coordinate diagram. Note that the intermediate carbenium ion is a shallow well on the free energy surface.



Also note from the reaction coordinate diagram that formation of a carbenium ion from H^+ and an alkene is an energetically uphill process. From the change in free energy, one sees that the equilibrium constant for formation of a carbenium ion from alkene and H^+ is small. Although the equilibrium lies far to the side of “alkene + H^+ ”, the catalyst provides an overall lower free energy pathway to product than would occur in the absence of catalyst. This situation is common. Catalysts generally work by providing a reaction pathway that is *different and lower in activation energy* than non-catalyzed pathways. In this case the key effect of the catalyst is to generate a thermodynamically unstable but *highly reactive* carbenium ion.

Appendix. Gallery of Some Donor and Acceptor Orbitals

Donor Orbitals		Acceptor Orbitals	
Cartoon Drawing	Quantum Calculation ^a	Cartoon Drawing	Quantum Calculation ^a
$\text{H}_3\text{C-Li}$  filled σ bond		H-F  empty σ^* -antibonding	
H_3N  lone pair		CH_3^+  empty p-orbital	
$\text{H}_2\text{C=CH}_2$  filled π bond		$\text{H}_2\text{C=O}$  empty π^* -antibonding	

^a Quantum calculations demonstrate the orbitals as contour plots. You may have seen contour lines on terrain maps where the lines represent changes in elevation. In these contour maps the lines represent changes in the wavefunction (orbital) values. The dashed lines represent areas of negative phase and the solid lines are positive phase. Contour and relief of an island are shown below.

